Dalton Transactions

RSC Publishing

PAPER

View Article Online
View Journal

Cite this: DOI: 10.1039/c3dt00065f

Synthesis and structures of calcium and strontium 2,4-di-*tert*-butylphenolates and their reactivity towards the amine co-initiated ring-opening polymerisation of *rac*-lactide†

Lawrence Clark,[a] Glen B. Deacon,*[b] Craig M. Forsyth,[b] Peter C. Junk,*[b,c] Philip Mountford,*[a] Josh P. Townley[b] and Jun Wang[b]

Calcium and strontium metals react with $Hg(C_6F_5)_2$ and 2,4-di-*tert*-butylphenol (H-DBP) in tetrahydrofuran (THF) and 1,2-dimethoxyethane (DME) to give $[Ca(DBP)_2(THF)_4]$ (**1**), $[Ca_2(DBP)_4(DME)_4(\mu\text{-DME})]$ (**2**), $[Sr_3(\mu\text{-DBP})_6(THF)_6]$ (**3**), and $[Sr_2(DBP)(\mu\text{-DBP})_3(DME)_3]$ (**4**). Compound **1** is a six coordinate *trans*-octahedral monomer, whereas in binuclear **2** two seven-coordinate Ca centres are bridged by a DME ligand. In **3** a central Sr is connected by three bridging DBP groups to each of two terminal $Sr(THF)_3$ moieties, all metal atoms being six coordinate. Compound **4** has one six- and one seven-coordinate Sr, bridged by three DBP ligands, the former Sr also having a terminal DBP and a bidentate DME ligand and the latter two DME ligands. Complexes **2** and **4** act as ring-opening polymerisation (ROP) catalysts for the benzyl alcohol or benzylamine co-initiated ROP *rac*-lactide forming atactic alcohol- or amine-terminated polylactide H-[PLA]-XBn (X = O or NH) with reasonable control of molecular weight *via* an activated monomer propagation mechanism. Kinetic studies for $BnNH_2$ found the unusual rate expression $-d[LA]/dt = k_{p(Ae)}[\mathbf{2} \text{ or } \mathbf{4}]_0[rac\text{-LA}]^2[BnNH_2]_0^{2.5}$ ($k_{p(Ca)} \approx 1.7 \times k_{p(Sr)}$). Preliminary studies suggest that $[Y(DBP)_3(THF)_2]$ also catalyses amine or alcohol co-initiated ROP by an activated monomer mechanism without loss of a phenoxide ligand.

Received 8th January 2013,
Accepted 13th February 2013

DOI: 10.1039/c3dt00065f

www.rsc.org/dalton

Introduction

Poly(lactide) (PLA) derived plastics are important renewable, biocompatible and biodegradable materials.[1] Studies of the ring-opening polymerisation (ROP, the preferred method of PLA synthesis from both an industrial and academic perspective) of the cyclic diester, lactide (LA) has attracted sustained interest over the last 15 years in particular.[2] Metal alkoxides of the type (L)M-OR (either previously isolated or generated *in situ*; L = supporting ligand set) are normally considered to be the optimum initiators since these generally give similar rates of initiation (rate constant k_i) and propagation (rate constant k_p). Similarly, alcohol co-initiators with organic catalysts have attracted recent attention.[2f] Alcohols can function as chain transfer agents (CTAs) with metal catalysts leading to the "immortal" ROP (iROP) of LA in which one H-[PLA]-OR polymer chain is formed per added ROH and grows continually through the ROP process.[2s] For metal complex-mediated ROP, in the absence of any added alcohol CTA, monomer enchainment almost always proceeds *via* the "coordination–insertion" mechanism (repeated insertion of LA into the growing $M\text{-}O_{PLA}$ chain of a metal complex). In the presence of an alcohol CTA under iROP conditions, propagation usually proceeds *via* coordination–insertion, but this is accompanied by fast exchange (rate constant k_{CT} where $k_{CT} \gg k_p$) between the metal-bound polymeryl chain and a free HO-terminated PLA chain. However, it is also possible that in the presence of ROH, propagation can proceed *via* the "activated monomer" mechanism in which ROH (where ROH is either the initial added alcohol or a HO-terminated PLA chain) externally attacks a metal-bound LA moiety with the metal acting as a Lewis acid catalyst.[2s,3] Mechanistic studies can in principle help distinguish between these possibilities.

Whereas there are numerous well-established examples of the synthesis of RO-terminated PLAs (H-[PLA]-OR) (with or without the use of CTAs), there are very few, good ROP-based

[a]*Chemistry Research Laboratory, Department of Chemistry, University of Oxford, Mansfield Road, Oxford OX1 3TA, UK. E-mail: philip.mountford@chem.ox.ac.uk*
[b]*School of Chemistry, Monash University, Clayton, Vic. 3800, Australia. E-mail: glen.deacon@monash.edu*
[c]*School of Pharmacy and Molecular Sciences, James Cook University, Townsville, Qld 4811, Australia. E-mail: peter.junk@jcu.edu.au*

†Electronic supplementary information (ESI) available: Further details of the ROP experiments and NMR tube scale experiments. CCDC 914477–914480. For ESI and crystallographic data in CIF or other electronic format see DOI: 10.1039/c3dt00065f

routes to amine (NRR′)-terminated PLA. Such methodologies could allow the use of functionalised amines and poly(amines) for the preparation of complex architectures such as block- or graft-copolymers, dendritic copolymers and star-shaped polymers.[1h] Metal amides (L)M-NR_2 often give poor control of molecular weight due to a mismatch of the rates of initiation and propagation, and a propensity to form cyclic PLAs.[4] Waymouth *et al.* have reported a stoichiometric organocatalytic method based on the insertion of carbenes into amine N–H bonds at 90 °C giving 85% conversion to PLA after 71 h.[5] Sn(octanoate)$_2$ was employed at high temperature under melt conditions (up to 150 °C and 72 h) to form PLA-functionalised amine-based dendrimers and star-polymers.[6] In this case one PLA chain forms per Sn–Oct bond and there is extensive transesterification.[7]

In a recent advance in this area, as shown in Scheme 1, we recently reported that yttrium dicationic (**I**), zwitterionic (**II**) and neutral amide (**III**) compounds can act as catalyst precursors for the amine co-initiated iROP of *rac*-lactide using primary or secondary amines.[8] For compounds **II** and **III**, amine-terminated, highly heterotactic PLA of the type H-[PLA]-NHRR′ with narrow polydispersities and well-controlled molecular weights were rapidly prepared at RT. Subsequently, we reported that several trivalent indium compounds were also effective for this process, although these required longer reaction times at RT (up to 1 week) or elevated temperatures.[9] Mechanistic studies[8,9] established the general mechanism in Scheme 1 whereby a number of equivalents of LA are rapidly ring-opened by a primary or secondary amine $RR'NH_2$ (RR′NH is typically benzylamine, $BnNH_2$, in most mechanistic studies to date) *via* an activated monomer-type process to form an amine-terminated alcohol **IV** which eventually forms amine-terminated PLA of the type H-[PLA]-NRR′. Where the relevant mechanistic studies were undertaken,[8] the propagation process was established as rate-limiting coordination–insertion coupled with fast (non rate-limiting) exchange between the free H-[PLA]-NRR′ moieties and the metal-bound ones of the propagating species (L)M-[PLA]-NRR′ (*i.e.*, iROP). Specifically, while the number average *molecular weights* (M_n) of the PLAs formed in Scheme 1 are controlled by the initial $[lactide]_0 : [RNH_2]_0$ ratio (one chain per R′RNH), the *rates* of propagation are *independent* of $[RNH_2]_0$ (*i.e.*, the concentration of polymeryl chains, [H-[PLA]-NRR′]).

As part of these studies we recently described the synthesis, structures and ROP behaviour of the lanthanoid(III) 2,4-di-*tert*-butylphenolate complexes $[Ln(DBP)_3(THF)_3]$ (Ln = Nd, Gd; DBP = $-OC_6H_3Bu^t_2$-2,4).[10] These complexes on their own were fast but poorly-controlled initiators for the ROP of *rac*-LA. However, use of an excess of $BnNH_2$ afforded well-controlled, amine co-initiated iROP (analogous results were obtained with BnOH). The very fast rates of propagation and the paramagnetic nature of the complexes precluded a detailed study, and a coordination–insertion mode of propagation was proposed based on our mechanistic studies for **I–III** (Scheme 1) and previous literature where alcohol co-initiators were employed with Ln-$(OAr)_3$ systems.[11]

During their recent studies of the alcohol co-initiated ROP of lactide using cationic main group catalysts supported by phenolate-poly(ether) ligands,[3] Carpentier and Sarazin briefly reported another example of $BnNH_2$ co-initiated ROP for a zinc system. Mechanistic studies were not carried out for the amine co-initiated ROP, but we were interested to note that detailed analysis of the corresponding alcohol co-initiated systems showed that in these divalent systems iROP proceeded by *activated monomer* propagation. Similarly, while this manuscript was in preparation, Miller *et al.* proposed an activated

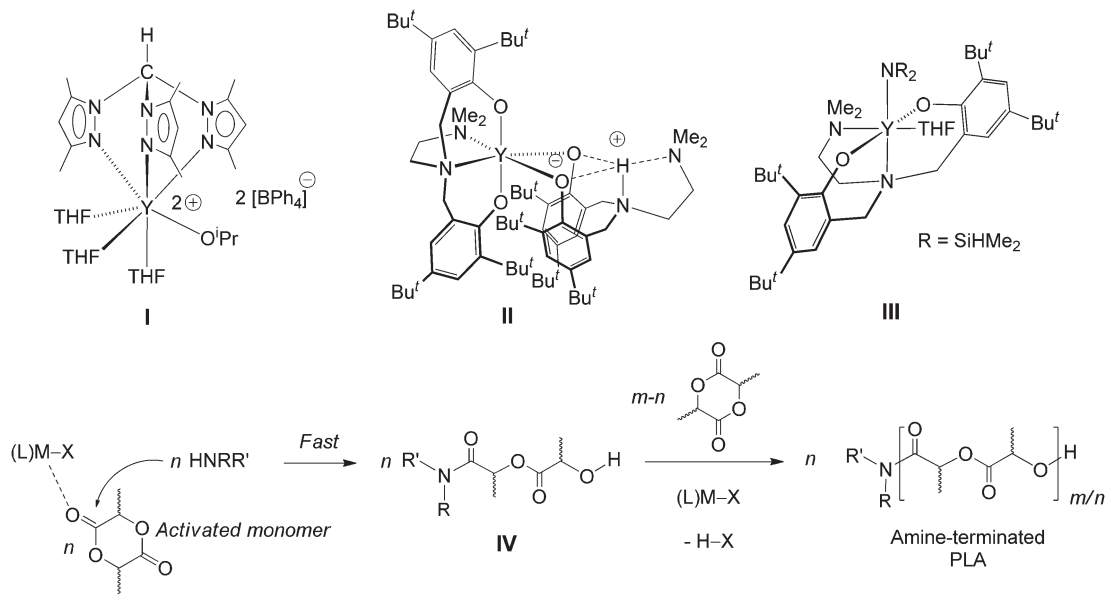

Scheme 1 Top: the first metal complexes (**I–III**) for fast and well-controlled amine co-initiated iROP of *rac*-LA. Bottom: general mechanism of initiation and propagation.[8]

monomer ROP process for alcohol co-initiated ROP catalysed by 2,6-di-*tert*-butyl-substituted magnesium and calcium phenolates although no kinetic analysis was presented in this case.[12]

We anticipated that extension of the trivalent lanthanoid complexes $[Ln(DBP)_3(THF)_3]$ to their divalent Ln^{II} counterparts would potentially be complicated by redox reactions as found previously.[13] On the other hand, use of alkaline earth (Ae) metal 2,4-di-*tert*-butylphenolates of the type $[Ae(DBP)_2(L)_n]$ (specifically for Ae = Ca and Sr since Ca^{2+}/Yb^{2+} and Sr^{2+}/Eu^{2+} have similar ionic radii.[14]) should provide access to their behaviour without any accompanying redox complications. In general terms the alkaline earth metals have attracted much recent interest with regard to their stoichiometric and catalytic reactivity.[15] From the point of view of ROP, these metals (with the exception of beryllium) are attractive owing to their low toxicity. In the last 10–12 years in particular, a range of supporting ligands have been employed to effect control of polymer molecular weights, microstructure, end groups and activity.[3,12,16] Most of these previous studies focussed on Mg and Ca systems, but more recently there has been increased interest in the ROP of lactones and lactide using molecular Sr initiators.[3,16q,t,u,w,x] Finally, with regard to compounds of the type $[Ae(DBP)_2(L)_n]$, we note that alkoxides and phenoxides of the heavy group 2 metals (Ca, Sr, Ba) show promising applications in other areas such as MOCVD and sol–gel processes.[17]

In this contribution we report the synthesis and solid state structures of new calcium and strontium bis(2,4-di-*tert*-butylphenolate) complexes together with a detailed study of their *rac*-lactide ROP capability, in particular using benzylamine as a co-initiator.

Results and discussion

Synthesis of calcium and strontium bis(2,4-di-*tert*-butylphenolate) complexes

Redox transmetallation/protolysis (RTP)[10,18] offers a simple route to alkaline earth phenoxides and offers a number of advantages over traditional metathesis, such as the simple one-pot synthesis, and avoiding the issue of halide or alkali metal retention.[17a,b,19] The use of a donor solvent often results in the isolation of heteroleptic complexes,[10,18] and the structural motif of the product can vary quite substantially depending on the steric demands of the coordinated solvent, which can be defined in terms of the steric coordination number (steric CN).[20] For the coordinating solvents THF and DME the steric coordination numbers are 1.21 and 1.78, respectively.[20] 2,4-Di-*tert*-butylphenol (H-DBP) was selected for these (and the previous studies of $[Ln(DBP)_3(THF)_3]$[10]) due to the steric bulk in just one *ortho*-position, the high solubility in organic solvent due to the *tert*-butyl substituents, the relative neglect of alkaline earth complexes of asymmetrically substituted phenoxides[15f,17a] and its relatively low cost. Unsymmetrical substitution of the phenolate may affect both bonding and bridging in complexes compared with the more commonly used symmetrical 2,6-disubstituted phenolates.

The complexes $[Ca(DBP)_2(THF)_4]$ (**1**), $[Ca_2(DBP)_4(DME)_4(\mu\text{-DME})]$ (**2**), $[Sr_3(\mu\text{-DBP})_6(THF)_6]$ (**3**), and $[Sr_2(DBP)(\mu\text{-DBP})_3(DME)_3]$ (**4**) were prepared by RTP reactions between an excess of freshly filed alkaline earth metal, $Hg(C_6F_5)_2$ and 2,4-di-*tert*-butylphenol (H-DBP) in tetrahydrofuran (THF) or 1,2-dimethoxyethane (DME) in the presence of a drop of added mercury for activation of the metal through surface amalgamation (Scheme 2). After a simple workup of filtration to remove mercury and excess Ae metal and evaporation to the point of crystallization, the products were obtained in good to excellent yield. Monitoring progress of the reactions was possible by ^{19}F NMR spectroscopy since $Hg(C_6F_5)_2$ and C_6F_5H have very different spectra.

An attempted reaction between Sr metal and H-DBP in THF in the presence of Hg metal failed. Accordingly, the reactions are considered to proceed by redox transmetallation giving highly reactive $[Ae(C_6F_5)_2(L)_n]$ (L = THF or DME) complexes (eqn (1)), which then undergo protolysis by the H-DBP (eqn (2)), a step driven by the large acidity difference between a phenol and C_6F_5H.[18c] There is experimental precedent for eqn (1) from the reactions of ytterbium or europium with $Hg(C_6F_5)_2$,[18c,21] and ^{19}F NMR evidence for formation of $Ae(C_6F_5)_2$ species have been obtained.[22] Attempted RTP reactions in diethyl ether failed although an analogous reaction of Nd metal giving $Nd_2(DBP)_6(OEt_2)_2$ has been reported.[10]

$$Ae + Hg(C_6F_5)_2 \rightarrow Ae(C_6F_5)_2 + Hg\downarrow \quad (1)$$

$$Ae(C_6F_5)_2 + 2\ \text{H-DBP} \rightarrow Ae(DBP)_2 + 2\ C_6F_5H \quad (2)$$

Complexes **1**–**4** were characterised in the solid state by X-ray crystallography (*vide infra*) and their C, H analyses were consistent with this composition for the bulk products (with the exception of **3** where loss of THF *in vacuo* leads to a lower than expected %C), as were their ^1H and ^{13}C NMR spectra. In the case of calcium complexes $[Ca(DBP)_2(THF)_4]$ (**1**) and $[Ca_2(DBP)_4(DME)_4(\mu\text{-DME})]$ (**2**), the ^1H NMR spectra in C_6D_6 show one type of DPB ligand environment as expected from the solid state structures (Scheme 2 and Fig. 1 and 2 below) with distinct signals for each of the ring protons. The *para*-Bu^t groups were also distinguished from the *ortho*-Bu^t groups, separated by approximately 0.2 ppm. The NMR spectra of $[Sr_3(\mu\text{-DBP})_6(THF)_6]$ (**3**) in C_6D_6 were more complex. At room temperature the ^1H and ^{13}C NMR spectra show two different DPB environments (1 : 1 ratio) in contrast to the solid state structure (Scheme 2 and Fig. 3 below) which shows only one type of phenoxide ligand environment. However at 70 °C, the ^1H NMR spectrum shows only a single set of DPB ligand resonances, indicative of fast exchange between the two environments. In THF-d_8 at 60 °C, a single set of DBP resonances is also observed, again either consistent with fast exchange of DBP environments or with conversion into monomeric $[Sr(DBP)_2(THF\text{-}d_8)_n]$. Overall these data suggest that one or more coordination geometries are available to **3** in solution,

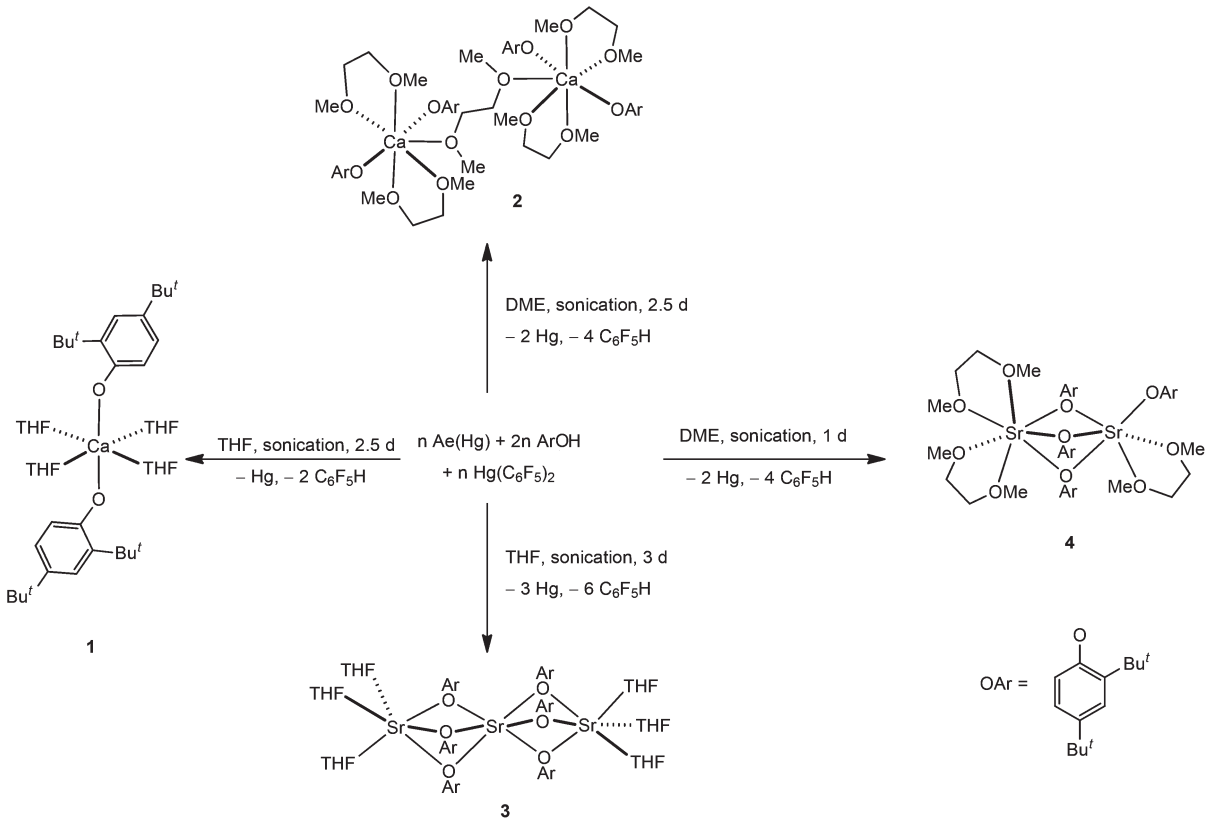

Scheme 2 Syntheses of compounds **1–4**. All reactions were performed at RT.

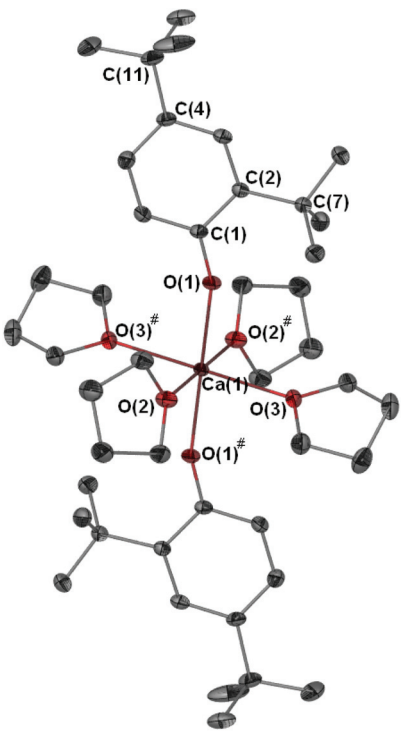

Fig. 1 Molecular structure of $[Ca(DBP)_2(THF)_4]$ (**1**). Hydrogen atoms omitted for clarity. Displacement ellipsoids drawn at 50% level.

consistent with the well known stereochemical non-rigidity of complexes of the larger alkaline earth metals.

The ^1H and ^{13}C NMR spectra of the unsymmetric $[Sr_2(DBP)(\mu\text{-}DBP)_3(DME)_3]$ (**4**) in C_6D_6 at RT shows only a single set of DBP (and DME) ligand resonances, indicative of rapid exchange between terminal and bridging phenolate ligands on the NMR timescale. At −80 °C in toluene-d_8, greater complexity is observed, consistent with the solid state structure. The ^1H NMR spectrum in THF-d_8 is analogous to that of **3** apart from the presence of free DME. These observations are consistent with substitution of DME by THF-d_8 in an excess of the latter although the nature of the species formed in solution (coordination number and nuclearity) is unknown.

Solid state structures of 1–4

The structures of the four complexes show remarkable variety, ranging from a six coordinate monomer **1**, through a seven coordinate DME-bridged dinuclear species **2**, to a trinuclear complex in which all phenoxide ligands are bridging **3**, and an unsymmetrical dinuclear structure with both six and seven coordinate metal atoms **4**. We discuss each in turn and selected distances and angles are collected in Table 1.

$[Ca(DBP)_2(THF)_4]$ (1). Compound **1** (Fig. 1) is monomeric with two *trans*-phenoxide and four equatorial THF ligands in a close to octahedral arrangement (O–Ca–O angles 86.70(4)–

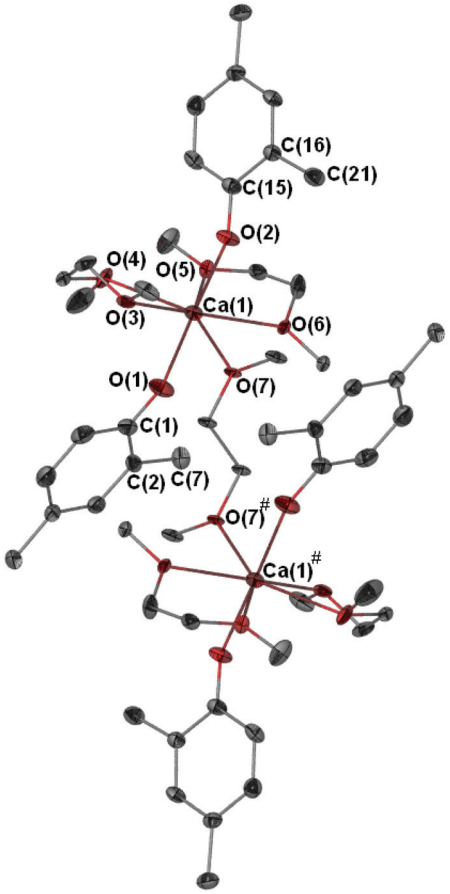

Fig. 2 Molecular structure of $[Ca_2(DBP)_4(DME)_4(\mu\text{-}DME)]$ (**2**). Hydrogen atoms and all primary carbons of Bu^t groups omitted for clarity. Displacement ellipsoids drawn at the 50% level.

93.30(4)°). Similar *trans*-$[Ca(OR)_2(THF)_4]$ structures are also observed for OR = $OC_6H_4Bu^t$-2 or $OSiPh_3$ and in one molecular component of $[Ca(OC_6H_3Pr^i_2\text{-}2,6)_2(THF)_4]\cdot[Ca(OC_6H_3Pr^i_2\text{-}2,6)_2(THF)_3]$.[23] By contrast, analogous alkoxides $[Ca(OR)_2(THF)_4]$ (R = CPh_3,[24a] $C(CF_3)_3$ [24b] and $CHCH_2$ (dimeric)[24c] have a *cis*

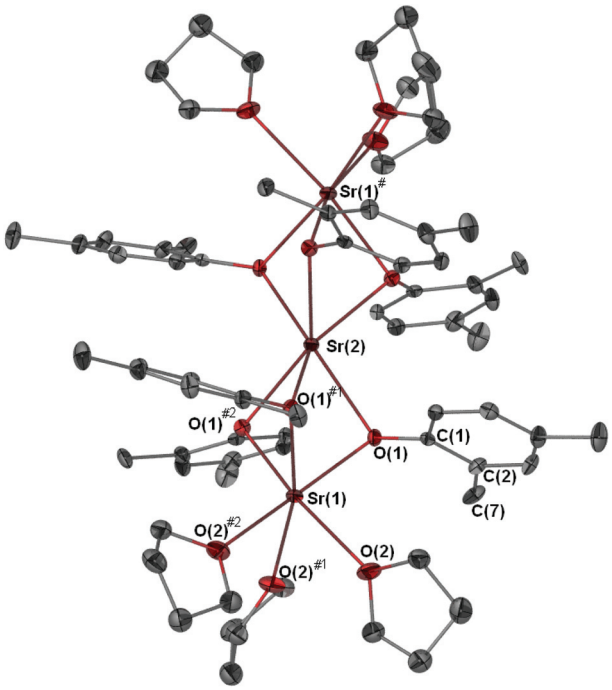

Fig. 3 Molecular structure of $[Sr_3(\mu\text{-}DBP)_6(THF)_6]$ (**3**). Hydrogen atoms, all primary carbons of Bu^t groups and lattice benzene molecules have been omitted for clarity. Displacement ellipsoids drawn at the 50% level.

Table 1 Selected bond lengths (Å) and angles (°) for complexes **1–4**

$[Ca(DBP)_2(THF)_4]$ (**1**)					
Ca(1)–O(1)	2.206(1)	Ca(1)–O(2)	2.407(1)	Ca(1)–O(3)	2.436(1)
O(1)–Ca(1)–O(2)	89.27(4)	O(2)–Ca(1)–O(3)	93.30(4)	O(1)–Ca(1)–O(3)	93.17(4)
Ca(1)–O(1)–C(1)	159.80(10)			Ca(1)···C(7)(*o*-Bu^t)	4.822(1)
$[Ca_2(DBP)_4(DME)_4(\mu\text{-}DME)]$ (**2**)					
Ca(1)–O(1)	2.192(3)	Ca(1)–O(2)	2.236(3)	Ca(1)–O(3)	2.518(3)
Ca(1)–O(4)	2.495(4)	Ca(1)–O(5)	2.526(3)	Ca(1)–O(6)	2.481(3)
Ca(1)–O(7)	2.462(3)	Ca(1)–O(1)–C(1)	159.5(3)	Ca(1)···C(7)(*o*-Bu^t)	4.798(4)
Ca(1)–O(2)–C(15)	141.5(2)	O(1)–Ca(1)–O(2)	177.34(11)	Ca(1)···C(21)(*o*-Bu^t)	5.031(4)
$[Sr_3(\mu\text{-}DBP)_6(THF)_6]$ (**3**)					
Sr(1)–O(1)	2.445(2)	Sr(1)–O(2)(THF)	2.650(2)	Sr(1)···C(7)(*o*-Bu^t)	4.723(3)
Sr(2)–O(1)	2.582(2)	Sr(1)–O(1)–C(1)	120.27(16)	Sr(2)···C(7)(*o*-Bu^t)	5.325(3)
Sr(1)–O(1)–Sr(2)	90.04(7)	Sr(2)–O(1)–C(1)	119.27(16)	Sr(1)···Sr(2)	3.556(0)
$[Sr_2(DBP)(\mu\text{-}DBP)_3(DME)_3]$ (**4**)					
Sr(1)–O(1)	2.340(2)	Sr(1)–O(2)	2.515(2)	Sr(1)–O(3)	2.539(2)
Sr(1)–O(4)	2.478(2)	Sr(1)–O(5)	2.769(3)	Sr(1)···C(7)(*o*-Bu^t)	4.826(4)
Sr(1)–O(6)	2.670(2)	Sr(2)–O(2)	2.457(2)	Sr(1)···C(21)(*o*-Bu^t)	4.913(3)
Sr(2)–O(3)	2.496(2)	Sr(2)–O(4)	2.507(2)	Sr(2)···C(21)(*o*-Bu^t)	5.037(3)
Sr(2)–O(7)	2.709(2)	Sr(2)–O(8)	2.669(3)	Sr(1)···C(35)(*o*-Bu^t)	4.950(4)
Sr(2)–O(9)	2.676(2)	Sr(2)–O(10)	2.632(2)	Sr(2)···C(35)(*o*-Bu^t)	5.120(4)
Sr(1)–O(1)–C(1)	152.0(2)	Sr(1)–O(2)–C(15)	100.70(18)	Sr(1)···C(49)(*o*-Bu^t)	4.751(4)
Sr(2)–O(2)–C(15)	145.4(2)	O(1)–Sr(1)–O(3)	179.01(8)	Sr(2)···C(49)(*o*-Bu^t)	5.256(4)
Sr(1)–O(3)–C(29)	131.87(19)	Sr(2)–O(3)–C(29)	111.63(19)	Sr(1)···Sr(2)	3.519(1)
Sr(1)–O(4)–C(43)	125.6(2)	Sr(2)–O(4)–C(43)	115.6(2)		

arrangement. The BHT (BHT = $OC_6H_2Bu^t_2Me$-2,4,6) analogue of **1**, namely $[Ca(BHT)_2(THF)_3]$, has only three THF ligands, consistent with the presence of two *ortho*-*tert*-butyl groups.[12] Whereas the Ca–O bond lengths (Table 1) are close to those of the $OC_6H_4Bu^t$-2 and $OSiPh_3$ analogues, the (Ar)C–O–Ca angle is substantially increased from the 2-*tert*-butylphenolate complex (146.95(13)°)[23] to **1** (159.8(1)°) (Table 1). Thus, the addition of the 4-Bu^t substituent has a significant structural effect. On the other hand, addition of a second *o*-Bu^t-substituent leads to five coordinate $[Ca(OAr)_2(THF)_3]$ complexes,[23,24a,25,29a] and this coordination number is also observed in the tris(THF) component of the 2,6-diisopropylphenolate above.[23]

$[Ca_2(DBP)_4(DME)_4(\mu\text{-}DME)]$ (2). The molecular structure of dinuclear complex **2** is shown in Fig. 2. The seven coordinate calcium atoms are ligated by *trans* phenoxide ligands (O(1)–Ca(1)–O(2) 177.34(11)°) and two chelating and one bridging DME in a pentagonal bipyramidal array (O(DME)–Ca–O(DME) between adjacent oxygens 65.13(11)–80.90(12)°). Similar bond lengths are observed for the two somewhat asymmetrically (Δ = 0.023/0.045 Å) chelating DME ligands (Table 1). Ca(1)–O(7) of the bridging DME is significantly shorter than Ca(1)–O(3,4,5,6) of the chelating DME ligands. In the related seven coordinate β-diketonato complex $[Ca_2\{(Bu^tCO)_2CH\}_4(\kappa^2\text{-}DME)_2(\mu\text{-}DME)]$, coordination of DME is far more unsymmetrical (Δ = 0.078 Å), and Ca–O(μ-DME) lies between the chelate values,[26] but the average Ca–O(DME) length is similar to that of **3**. For the phenolate ligands, Ca(1)–O(2) is significantly longer than Ca(1)–O(1), the Ca–O–C angle is more bent for the O(2) ligand, and the Ca(1)···C(21)(*o*-Bu^t) distance is longer than Ca(1)···C(7)-(*o*-Bu^t) (Table 1), all consistent with the greater crowding of the O(2) ligand. The aromatic ring of the phenolate is only 19.63(7)° out of the Ca(1)O(1,2,7) plane whereas that of the O(1) phenolate is rotated by 78.80(12)° thereby reducing the steric effect of the *o*-Bu^t group. Despite the coordination number differences, the Ca(1)–O(DBP) bond lengths of **2** are comparable with those of **1**, but the Ca(1)–O(DME) values are greater than Ca(1)–O(THF) bond lengths by almost that (0.06 Å) expected for the difference in ionic radii.[14] By contrast with **2**, somewhat bulkier $OC_6H_3R_2$-2,6 (R = Me, Pr^i) or BHT ligands give mononuclear six coordinate $[Ca(OAr)_2(DME)_2]$ complexes[12,27] (steric coordination numbers: 1.59 (R = Me),[20] 1.70 (R = Pr^i),[20] 1.38 (DBP)[10]). A bridging DME is surprising given the propensity of phenoxide ligands to bridge,[17a] for example in $[Ca_2(OC_6H_2Me_3\text{-}2,4,6)_2(\mu\text{-}OC_6H_2Me_3\text{-}2,4,6)_2(\kappa^2\text{-}DME)_2(\kappa^1\text{-}DME)_2]$.[28a] However, the present results can be rationalised in terms of the different steric requirements of THF and DME.[20] Thus, the sum of the ligand steric coordination numbers is 7.60 for six coordinate **1** and 7.21 for seven coordinate **2**. Chelation of a third DME to give eight coordinate $[Ca(DBP)_2(DME)_3]$ would result in a sterically more strained 8.10.

$[Sr_3(\mu\text{-}DBP)_6(THF)_6]$ (3). The unusual trinuclear complex **3** (Fig. 3) crystallises in the space group $R\bar{3}c$ all three DBP ligands are crystallographically equivalent. An initial determination established the connectivity, but was of a low precision. A higher quality structure was then obtained for a benzene solvate using synchrotron radiation. Each six coordinate terminal Sr atom is linked to the six coordinate central strontium by three bridging 2,4-di-*tert*-butylphenolate ions and they are capped by three THF ligands. Unusually there are no terminal phenoxide ligands. The stereochemistry of the central Sr(2) is a symmetrical triangular prism, whilst the triangle of O(THF) donors (O(2), O(2)#1, O(2)#2) is twisted with respect to the O(1), O(1)#1, O(1)#2 triangle by 41.81(7)°, resulting in triangular antiprismatic stereochemistry for Sr(1, #1). This unusual structural motif has nevertheless been previously encountered in $[Eu_3(OC_6H_3Me_2\text{-}2,6)_6(THF)_6]$,[28b] and the isotypic $[M_3(OC_6H_2Me_2\text{-}2,4,6)_6(THF)_6]$ (M = Sr, Ba,[28a] Eu[28c]), in all of which the phenoxide ligands are considerably bulkier (steric CN ≥ 1.59) than DBP (Steric CN 1.38). In **3**, the sum of the steric coordination numbers at Sr(2) is 8.28 and at Sr(1) is 7.77, by contrast with the very large 9.54 (or greater) for the central metal of the reported complexes.[28] In the present high symmetry complex the Sr–O(DBP) bond length to the less crowded Sr(1) is much shorter (0.14 Å) than to the more crowded Sr(2) (Table 1), as also observed for the reported analogues.[28] In $[Sr_3(OC_6H_2Me_2\text{-}2,4,6)_6(THF)_6]$, which is less symmetrical, the ranges of Sr(2)–OAr (2.516(4)–2.616(4) Å), Sr(1)–OAr (2.408(4)–2.458(4) Å, Sr(1)–O(THF) (2.597(4)–2.684(4) Å) encompass the corresponding values for **3**, but, surprisingly for a bulkier phenoxide, the averages are not larger than the values for **3**.

$[Sr_2(DBP)(\mu\text{-}DBP)_3(DME)_3]$ (4). Complex **4** (Fig. 4) crystallises in the space group $P2_1/n$ and is dinuclear and unsymmetrical with three bridging phenoxides, a terminal phenoxide and a chelating DME on Sr(1), but two chelating DME ligands and no terminal DBP on Sr(2). Consequently Sr(1) is six coordinate,

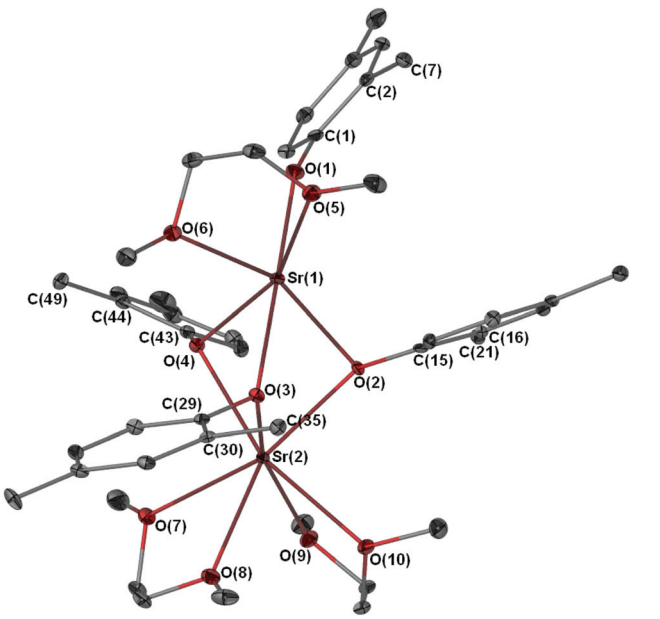

Fig. 4 Molecular structure of $[Sr_2(DBP)(\mu\text{-}DBP)_3(DME)_3]$ (**4**). Hydrogen atoms and all primary carbons of Bu^t groups omitted for clarity. Displacement ellipsoids drawn at the 50% level.

but Sr(2) seven. The former has distorted octahedral stereochemistry, with the terminal and one bridging DBP ligands in apical positions (O(1)–Sr(1)–O(3) angle = 179.01(8)°), whilst the arrangement at Sr(2) is irregular. Analogous connectivity is observed in $[Eu_2(OC_6H_3Me_2\text{-}2,6)_4(DME)_3]$[27a] with a bulkier phenoxide, but Eu^{2+} and Sr^{2+} have similar ionic radii.[14] Furthermore, the structural motif of three bridging and one terminal phenoxide is being increasingly observed in Sr, Eu^{II} and Ba chemistry, *e.g.* in a *N*-methylimidazole solvated europium(II) 2,6-dimethylphenolate,[29a] and also in the unsolvated $[M_2(ODPP)_4]$ (ODPP = $OC_6H_3Ph_2$-2,6); M = Sr, Ba,[29b] Eu,[29c] $[MEu(ODPP)_4]$ (M = Sr, Ba), and $[SrBa(ODPP)_4]$,[30] where intramolecular π-Ph···M coordination occurs in place of donor solvent coordination as in **4**. As expected, the terminal Sr–O bond length is the shortest (Table 1) but, unexpectedly two of the three pairs of bridging Sr–O bond lengths are larger to the six coordinate Sr atom, which is also less crowded (Σ steric CN 7.30 Sr(1); 7.72 Sr(2)). In the Eu analogue, all $OC_6H_3Me_2$-2,6 ligands form longer bridges to the six coordinate Eu.[27a] Likewise, average Sr–O(DME) bond lengths are larger for six coordinate Sr(1). Overall, average Sr–O bond lengths in all categories are similar to those of $[Eu_2(OC_6H_3Me_2\text{-}2,6)_4(DME)_3]$ despite greater steric crowding (steric CN, 8.14, 8.56 at six and seven coordinate Eu atoms) but Eu–O bond lengths cover a wide range. The asymmetry in the bridging in **4** is less marked than in the more crowded **3**. As the terminal Sr–O bond length of **4** is lengthened from the corresponding Ca–O bond length of **1** and **2** by significantly less than expected from ionic radii (0.18 Å),[14] there must be significant steric stress in the calcium complexes.

We have earlier shown that in $[Ln(DBP)_3(THF)_3]$ complexes, the Ln–O–C angles of the coordinated phenoxides become more bent as the Ln^{3+} ion size contracts, thereby offsetting increased steric stress by avoiding a decrease in the Ln–C(*o*-Bu^t) distance.[10] For complex **1**, Ca(1)–O(1)–C(1) (159.80(10)° is somewhat less bent than <La–O–C>(155.8°)[17] and Ca–C(*o*-Bu^t) (4.822(1) Å) is slightly shorter than <La–C(*o*-Bu^t)>(4.94 Å) with Ca^{2+} slightly smaller than La^{3+} (1.00/1.03 for six coordination).[14] In the case of **2**, Ca(1)–O(2)–C(15) of ligand 2 is more bent than Ca(1)–O(2)–C(7) of ligand 1 (Table 1) and the quaternary carbon of the Bu^t group of ligand 2 is further from Ca(1), though ligand O(1) avoids steric problems by twisting of the aryl group (above). For **3** with solely bridging phenoxides, the Sr(1,2)–O(1)–C(1) angles are shallow, consequent on bridging, with considerable variation in the Sr(1,2)–C(7)-(*o*-Bu^t) distance owing to unsymmetrical bridging. With the terminal ligand of **4**, Sr(1)–O(1)–C(1) is more bent than Ca(1)–O(1)–C(1) of **1**, but the distances to the quaternary carbon of *o*-Bu^t are comparable.

Ring-opening polymerisation of *rac*-lactide

One of our main objectives in this study was to determine the effectiveness of alkaline earth DPB complexes as initiators/catalysts for the ROP of lactide, in particular using amine co-initiators which have not yet been established for the alkaline earth metals. $BnNH_2$ was used as the representative amine for comparison with previous studies (and has been shown to provide the best performance so far).[3a,8–10] ROP experiments were performed in a glove-box in THF at RT using thoroughly purified *rac*-LA ($[rac\text{-LA}]_0$ = 0.69 M). Aliquots were taken at various intervals, quenched with non-dried (as-supplied) THF and analysed by ^{1}H NMR spectroscopy (% conversion and end group and tacticity analysis). Number average and weight average molecular weights (M_n and M_w) were determined using gel permeation chromatography (GPC; polystyrene standards with appropriate Mark–Houwink corrections for PLA in THF at 30 °C[31]). MALDI-ToF mass spectrometry was used for additional polymer analysis for PLAs with M_n up to *ca.* 3–4 × 10^3 g mol^{-1}. Full details are given in the Experimental section.

Preliminary studies. The results of initial ROP screening experiments using $[Ca_2(DBP)_4(DME)_4(\mu\text{-DME})]$ (**2**) and $[Sr_2(DBP)(\mu\text{-DBP})_3(DME)_3]$ (**4**) (and also with BnOH and $BnNH_2$ co-initiators) are summarised in Table 2. Additional preliminary studies found that **3** performed similarly to **4** but that for **3** the agreement between calculated and measured M_n values were slightly less good and the polydispersity indices (PDIs,

Table 2 Polymerisation of *rac*-LA using $[Ca_2(DBP)_4(DME)_4(\mu\text{-DME})]$ (**2**) and $[Sr_2(DBP)(\mu\text{-DBP})_3(DME)_3]$ (**4**) as initiators/catalysts and BnOH or $BnNH_2$ as co-initiators[a]

Entry	Complex/co-initiator	$[rac\text{-LA}]_0$: $[\text{Co-initiator}]_0$	Time (min)	Conv.[b] (%)	M_n (calcd) (g mol^{-1})	M_n (GPC)[c] (g mol^{-1})	M_w/M_n [c]
1	**2**[d]	[d]	30	73	[i]	[i]	[i]
2	**2**[d]	[d]	150	89	3200[e] 12 800[f]	4050	2.6
3	**4**[d]	[d]	30	51	[i]	[i]	[i]
4	**4**[d]	[d]	150	86	3100[e] 12 400[f]	13 200[j]	1.5[j]
5	**2**/$BnNH_2$	20 : 1	10	95	2850[g]	3070	1.8
6	**4**/$BnNH_2$	20 : 1	10	96	2870[g]	3320	2.0
7	**2**/BnOH	20 : 1	10	95	2850[h]	3000	1.8
8	**4**/BnOH	20 : 1	10	96	2880[h]	3010	1.8

[a] $[rac\text{-LA}]_0$: [**2** or **4**]$_0$ = 100 : 1, 2 mL THF, $[rac\text{-LA}]_0$ = 0.69 M, RT. [b] Measured by ^{1}H NMR in $CDCl_3$. [c] Measured by GPC against polystyrene standards using the appropriate Mark–Houwink corrections for PLA in THF at 30 °C.[31] [d] No co-initiator added. [e] M_n(calcd) for one PLA chain per Ae–DBP group = (Conv.(%) × 144.1)/4. [f] M_n(calcd) for one chain per complex = (Conv. (%) × $[rac\text{-LA}]_0$: $[\text{Complex}]_0$ × 144.1). [g] M_n(calcd) for one PLA chain per added $BnNH_2$ = (Conv. (%) × $[rac\text{-LA}]_0$: $[BnNH_2]_0$ × 144.1 + 107.2). [h] M_n(calcd) for one PLA chain per added BnOH = (Conv. (%) × $[rac\text{-LA}]_0$: $[BnOH]_0$ × 144.1 + 108.1). [i] Not measured. [j] Bimodal distribution, major peak area measured (87%).

M_w/M_n) were slightly larger. Since work-up of **3** appeared to result in some THF loss (*vide supra*) it was felt that the DME adduct **4** was more consistently well-defined on the bulk preparative scale. For best comparison with **4**, the DME adduct **2** was chosen as the calcium system.

In the case of **2** with $[rac\text{-LA}]_0:[\text{Complex}]_0 = 100:1$, 89% conversion of monomer to PLA was achieved in 150 min (entry 2), with intermediate aliquots at 30 and 60 min showing 73% and 80% conversion, respectively. The corresponding reaction with **4** proceeded over a similar timescale and 86% conversion of monomer to PLA was achieved in 150 min (entry 4). Intermediate aliquots were taken at 30, 60 and 120 min and showed 51%, 70% and 83% conversion, respectively. For the PLA obtained with **2**, the experimental (GPC) molecular weight, M_n(GPC), = 4050 g mol^{-1}, consistent with one chain forming for each Ca–DBP moiety (M_n(calcd) = 3200 g mol^{-1}), whereas in the case of **4** M_n(GPC) = 13 200 g mol^{-1} was more consistent with one PLA per molecule of **4** (M_n(calcd) = 12 400 g mol^{-1}) than for each Sr–DBP unit (M_n(calcd) = 3100 g mol^{-1}). At first sight the M_n(GPC) values appear to correlate with the solid state structures of **2** and **4** (Scheme 2) assuming that only the terminal DBP ligands can act as a initiators (*i.e.*, in **2**, all four DBP ligands are terminal whereas in **4** there is one terminal DBP ligand per dinuclear complex). However, the broad PDIs (2.6 and 1.5) are indicative of a poorly controlled process. In addition no –DBP end-groups could be detected in either the ^{1}H NMR or MALDI-ToF mass spectra, the latter showing only cyclic PLA arising from transesterification side reactions, along with an unassignable minor secondary distribution. Care should therefore be taken in drawing conclusions between the solid state structures of **2** and **4** and the experimental molecular weights observed in Table 2. With the absence of evidence for the participation of a conventional initiating group, initiation by trace water or lactic acid cannot be ruled out, despite the rigorous purification of the solvent and *rac*-LA.

Incorporation of either $BnNH_2$ (entries 5 and 6) or BnOH (entries 7 and 8) into the ROP experiments with $[rac\text{-LA}]_0:[BnNH_2 \text{ or } BnOH]_0:[\mathbf{2} \text{ or } \mathbf{4}]_0 = 100:5:1$ gave a considerably faster polymerisation system in all cases with >95% conversion to amine (H-[PLA]-NHBn) or alcohol (H-[PLA]-OBn) terminated PLA within 10 min. The M_n(GPC) values are consistent with one chain forming per added co-initiator with M_n(GPC) in the range 3000–3320 g mol^{-1} and M_n(calcd) in the range 2850–2880 g mol^{-1}. The ^{1}H NMR spectra were consistent with the expected HOC(H)Me– and –C(O)XBn (X = NH or O) end groups. MALDI-ToF analysis (*e.g.* Fig. S1† of the ESI) also confirmed the expected chain ends but in addition revealed the presence of cyclic PLA (presumably due to intramolecular transesterification processes). The separation of $\Delta(m/z)$ = 72 g mol^{-1} between the adjacent peak envelopes in both the linear and cyclic PLAs in the mass spectra is also indicative of extensive transesterification processes. The PDI values of 1.8–2.0 for these PLAs are consistent with the concurrent formation of cyclic PLAs and transesterification reactions. Again no evidence of –DBP terminated PLAs were found by NMR or MALDI-ToF analysis.

Overall the data in Table 2 show that **2** and **4** alone are poor initiators but that use of $BnNH_2$ or BnOH co-initiators considerably improve the performance. At first sight the $BnNH_2$ co-initiator is acting in a manner analogous to that found previously (Scheme 1) and in the remainder of this paper we address this aspect in detail. The PLA formed with **2–4** showed no heterotactic or isotactic enrichment, the polymers being atactic in all cases as determined from the selectively homonuclear decoupled ^{1}H NMR spectra of the polymers.[32]

Lactide and co-initiator loading studies. Building on entry 5, Table 2, Further ROP experiments were performed where $[rac\text{-LA}]_0:[\mathbf{2}]_0$ was increased from 100 : 1 to 500 : 1 equiv., holding $[BnNH_2]_0:[\mathbf{2}]_0$ constant at 5 : 1 and $[rac\text{-LA}]_0$ = 0.69 M. These data are plotted in Fig. 5 as M_n(GPC) *vs.* $([rac\text{-LA}]_0-[rac\text{-LA}]_t):[\mathbf{2}]_0$. The line of least-squares best fit gave a gradient 27(1) g mol^{-1} (R^2 = 0.991) in excellent agreement with the expected value of 28.8 g mol^{-1} (*i.e.* M_R of $[rac\text{-LA}]/5$ = 144.1/5 g mol^{-1}) for one chain growing per $BnNH_2$ (5 polymer chains growing per equiv of **2**). Fig. 6 shows plots of M_n(GPC) *vs.* $([rac\text{-LA}]_0-[rac\text{-LA}]_t):[BnNH_2]_0$ for the ROP of *rac*-LA for a related second series of runs where $[rac\text{-LA}]_0:[\mathbf{2} \text{ or } \mathbf{4}]_0 = 200:1$, and 3, 5, 7 or 10 equiv. of $BnNH_2$ co-initiator were added. In these plots the expected line of least-squares fit has a gradient of 144 g mol^{-1} (*i.e.* M_R of [*rac*-LA]) for one H-[PLA]-NHBn chain forming per equivalent of amine. In each case the experimental gradient of the least-squares fitted line was slightly lower than expected (133(6) g mol^{-1} (R^2 = 0.950) for **2** and 122(6) (R^2 = 0.954) g mol^{-1} for **4**) but still in good agreement and comparable to other systems we have studied.[8a,9]

NMR tube scale mechanistic studies. To gain additional insight into the $BnNH_2$ or BnOH co-initiated ROP of *rac*-LA a series of NMR tube scale experiments were carried out in C_6D_6 and THF-d_8. As expected on Brønsted acidity trends for amines, aliphatic alcohols and phenols[33] neither BnOH nor $BnNH_2$ (4 equiv.) reacted with **2** or **4** to eliminate H-DBP,

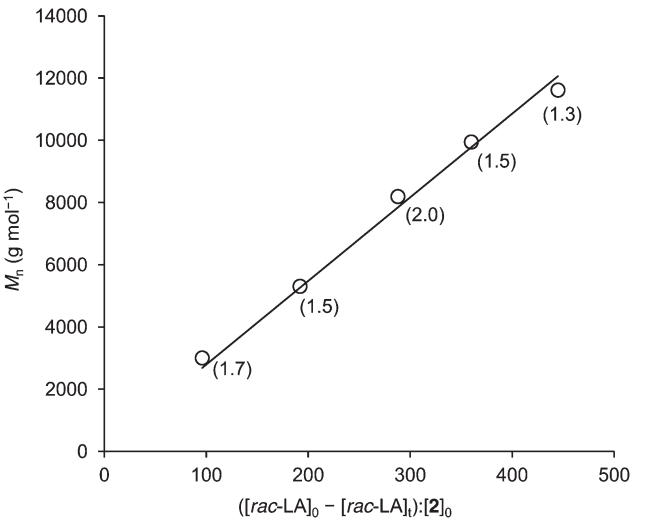

Fig. 5 M_n(GPC) *vs.* $([rac\text{-LA}]_0-[rac\text{-LA}]_t):[\mathbf{2}]_0$, $[rac\text{-LA}]_0:[\mathbf{2}]_0$ = 100, 200, 300, 400 or 500, using **2** and 5 equiv. $BnNH_2$ as co-initiator. PDIs are given in parentheses and intercept was set to 107.2 g mol^{-1} (M_R $BnNH_2$).

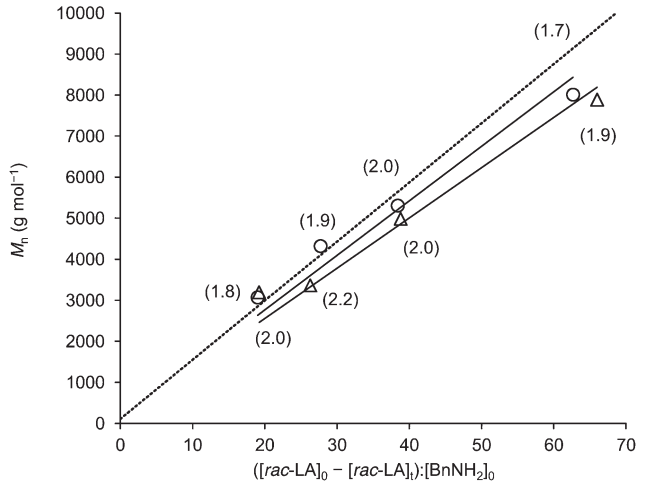

Fig. 6 M_n(GPC) *vs.* ([*rac*-LA]$_0$–[*rac*-LA]$_t$) : [BnNH$_2$]$_0$ for the ROP of *rac*-LA ([*rac*-LA]$_0$: [**2** or **4**]$_0$ = 200 : 1) using [Ca$_2$(DBP)$_4$(DME)$_4$(μ-DME)] (**2**) (circles) or [Sr$_2$(DBP)(μ-DBP)$_3$(DME)$_3$] (**4**) (triangles) and 3, 5, 7 or 10 equiv. BnNH$_2$ as co-initiator. The numbers in parentheses are the PDIs and the intercepts were set to 107.2 g mol^{-1} (M_R BnNH$_2$). The dashed line represents M_n(calcd) based on [*rac*-LA]$_0$: [BnNH$_2$]$_0$ = 200 : *n*.

although they appear to compete with DME as a donor ligand based on the changes in the chemical shifts of the respective resonances. When *rac*-LA (20 equiv.) was added to the mixtures (*cf.* Fig. S2† of the ESI) there was complete consumption of both the lactide and the BnOH or BnNH$_2$, and concomitant formation of H-[PLA]-XBn (X = NH or O) oligomer. This is consistent with results in Table 2 (entries 5–8) and Fig. 5 and 6 that the co-initiator is consumed rapidly at the beginning of the reaction in order to generate the multiple H-[PLA]-XBn PLA chains (*cf.* Scheme 1) which are then able to propagate.[8a,9]

Interestingly, while quantitative displacement of DME from each metal complex occurred upon formation of H-[PLA]-XBn (as judged by comparison of the chemical shifts with those for free DME in the same solvent), there was no formation of the phenol H-DBP which would be expected if propagation proceeded by the coordination–insertion mechanism and *in situ* formed (L)Ae-[PLA]-XBn units. These results imply that ROP catalysed by **2** and **4** in the presence of BnNH$_2$ or BnOH may proceed *via* an activated monomer mechanism, consistent with recent proposals by Carpentier *et al.*[3] and Miller *et al.*[12] This was supported by further NMR tube scale experiments (*cf.* Fig. S3† of the ESI) in which up to 4 equiv. of isolated benzyl amine-terminated PLA macromonomer (H-[*rac*-LA]$_{10}$-NHBn, M_n = 1600 g mol^{-1}, PDI = 1.11), independently prepared using Y(O$_2$N^{NMe2})(HO$_2$N^{NMe2}),[8a] were successively added to **2** or **4**. ^{1}H NMR analysis again showed no liberation of H-DBP, but DME was displaced showing that the PLA chains can act as ligands. Addition of 20 equiv. *rac*-LA showed that each system was active for ROP (Fig. S3†) as judged by the immediate consumption of *rac*-LA and the increase of relative intensity of the H-[*rac*-LA]$_n$-NHBn main chain resonances.

Kinetic studies: metal and LA dependences. The experiments described above indicate that ROP of *rac*-LA using BnNH$_2$ and either **2** or **4** proceeds broadly according to Scheme 1 with initial, very rapid ring-opening of lactide by all the amine to form H-[*rac*-LA]-NHBn. This is followed by iROP type propagation catalysed by the metal complex in an activated monomer type mechanism. In this case a rate law of the type shown in eqn (3) should apply[2s,3b] where −d[*rac*-LA]/d*t* is the rate of monomer consumption and $k_{p(Ae)}$ is the propagation rate constant for **2** ($k_{p(Ca)}$) or **4** ($k_{p(Sr)}$).

$$-\mathrm{d}[\textit{rac}\text{-LA}]/\mathrm{d}t = k_{p(Ae)}[\mathbf{2}\text{ or }\mathbf{4}]_0{}^a[\textit{rac}\text{-LA}]^b[\mathrm{BnNH_2}]_0{}^c \qquad (3)$$

Initial studies focused on the benzylamine co-initiated ROP of *rac*-LA using **4** as the catalyst and a loading of [*rac*-LA]$_0$: [BnNH$_2$]$_0$: [**4**]$_0$ = 400 : 5 : *n*. Runs were performed where the initial *rac*-LA and BnNH$_2$ concentrations were held constant ([*rac*-LA]$_0$: [BnNH$_2$]$_0$ = 400 : 5, 0.69 M and 8.6 × 10^{-3} M respectively) and the relative concentration of **4** was increased from *n* = 0.5 to 2.5 molar equiv. with respect to this. A representative % Conversion *vs.* Time plot for the run with [*rac*-LA]$_0$: [BnNH$_2$]$_0$: [**4**]$_0$ = 400 : 5 : 1.5 is shown in Fig. 7 together the corresponding second-order plot modelling consumption of *rac*-LA for this experiment. A summary of key data is given in Table 3.

Plots of 1/[*rac*-LA]$_t$ *vs.* Time (*e.g.*, Fig. 8, left) were linear over all concentrations of **4** assessed, indicating that the polymerisation reaction proceeded with a second-order dependence in [*rac*-LA]. The gradients of the fitted lines in Fig. 8 afford the apparent second-order rate constants, $k_{app(Sr)}$ in each case (where $k_{app(Sr)} = k_{p(Sr)}[\mathbf{4}]_0{}^a[\mathrm{BnNH_2}]_0{}^c$, assuming that: (i) the concentration of growing H-PLA-NHBn chains is equivalent to [BnNH$_2$]$_0$; (ii) the concentration of the actual catalyst is equal to [**4**]$_0$; (iii) both remain constant throughout the reaction). The 2nd order dependence on [*rac*-LA] is unusual but not unprecedented.[8a,9,34,35] A plot of $k_{app(Sr)}$ *vs.* [**4**]$_0$ in the range molar equiv. [**4**]$_0$ = 0.5–2.5 was linear (Fig. 8, right) showing a first order dependence of $k_{app(Sr)}$ on [**4**]$_0$. Thus rate of propagation (eqn (3)) is proportional to [*rac*-LA]^2[**4**]$_0$, and from Fig. 8 (right) $k_{p(Sr)}[\mathrm{BnNH_2}]_0{}^c$ = 182(5) M^{-2} min^{-1}.

Further runs were performed where the molar equiv. of strontium *centres* (= 2 × [**4**]$_0$) were increased to exceed the number of growing polymer chains ([*rac*-LA]$_0$: [BnNH$_2$]$_0$: [**4**]$_0$ = 400 : 5 : 3.0, 400 : 5 : 4.0 and 400 : 5 : 5.0).[36] As shown in Fig. 8 (right) and Table 3, $k_{app(Sr)}$ increased only marginally after the 400 : 5 : 2.5 run in this region demonstrating kinetic saturation. In other words, propagation became limited by the number of propagating chains (*i.e.*, [BnNH$_2$]$_0$) rather than the availability of catalytic sites.

Molecular weight data were measured for selected experiments (Table 3 and Fig. 9). In general, the calculated and measured M_n of early aliquots taken from the reaction mixture were in reasonable agreement, but as the reaction progressed experimental molecular weights began to diverge from those expected. Fig. 9 (left) shows M_n(GPC) data and PDI for the run, [*rac*-LA]$_0$: [BnNH$_2$]$_0$: [**4**]$_0$ = 400 : 5 : 1.5 (at completion, M_n(calcd) = 9910 g mol^{-1}, M_n(GPC) = 7040 g mol^{-1} and PDI = 1.51, entry 9, Table 3). The lower than calculated M_n(GPC) at

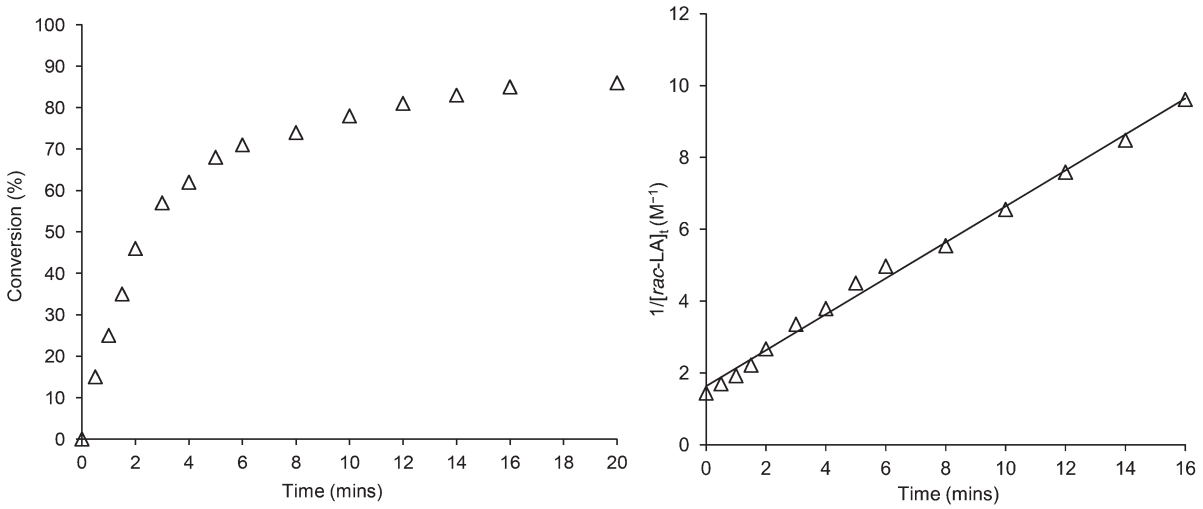

Fig. 7 Conversion *vs.* time profile (left) and second-order rate plot (right) for the run $[rac\text{-LA}]_0 : [BnNH_2]_0 : [\mathbf{4}]_0 = 400 : 5 : 1.5$ with $[rac\text{-LA}]_0 = 0.69$ M. $k_{app(Sr)} = 0.501(11)$ ($R^2 = 0.994$) M^{-1} min^{-1}, vertical-axis intercept = 1.63(8) M^{-1} (expected value = $1/[rac\text{-LA}]_0 = 1.44$ M^{-1}).

Table 3 Apparent second-order rate constants (k_{app}) and molecular weight data from the metal dependence determination experiments for $[Ca_2(DBP)_4(DME)_4(\mu\text{-DME})]$ (**2**) and $[Sr_2(DBP)(\mu\text{-DBP})_3(DME)_3]$ (**4**)

Entry	Complex	$[rac\text{-LA}]_0 : [BnNH_2]_0 : [\mathbf{2}$ or $\mathbf{4}]_0$ [a]	$k_{app(Ae)}$ [b] (M^{-1} min^{-1})	R^2 [b]	Conv.[c] (%)	M_n (calcd)[c] (g mol^{-1})	M_n (GPC)[d] (g mol^{-1})	M_w/M_n [d]
1	**2**	400 : 5 : 0.5	0.279(8)	0.994	[e]	[e]	[e]	[e]
2	**2**	400 : 5 : 1.0	0.534(12)	0.997	87	10 140	8880	1.35
3	**2**	400 : 5 : 1.5	0.897(22)	0.995	86	10 020	8200	1.36
4	**2**	400 : 5 : 2.5	1.323(52)	0.982	80	9330	6710	1.46
5	**2**	400 : 5 : 4.0	1.606(71)	0.981	86	10 020	6350	1.37
6	**2**	400 : 5 : 5.0	1.556(53)	0.986	[e]	[e]	[e]	[e]
7	**4**	400 : 5 : 0.5	0.136(5)	0.986	[e]	[e]	[e]	[e]
8	**4**	400 : 5 : 1.0	0.281(11)	0.984	80	9330	7140	1.66
9	**4**	400 : 5 : 1.5	0.501(11)	0.994	85	9910	7040	1.51
10	**4**	400 : 5 : 2.0	0.671(11)	0.997	76	8870	7550	1.70
11	**4**	400 : 5 : 2.5	0.759(23)	0.991	[e]	[e]	[e]	[e]
12	**4**	400 : 5 : 3.0	0.780(29)	0.986	82	9560	7730	1.51
13	**4**	400 : 5 : 4.0	0.813(49)	0.975	74	8640	5790	1.36
14	**4**	400 : 5 : 5.0	0.805(45)	0.967	88	10 250	5570	1.44

[a] $[rac\text{-LA}]_0 : [BnNH_2]_0 = 400 : 5$, $[rac\text{-LA}]_0 = 0.69$ M, THF, RT. [b] Apparent second-order rate constants ($k_{app(Ae)} = k_{p(Ae)}[\mathbf{2}$ or $\mathbf{4}]_0[BnNH_2]_0^c$) for consumption of *rac*-LA with standard error and R^2 determined by linear regression analysis. [c] Reactions monitored by ^1H NMR ($CDCl_3$) sampling; all quoted conversions refer to the last point where M_n(GPC) was determined. M_n(calcd) = (Conv. (%) × $[rac\text{-LA}]_0 : [BnNH_2]_0$ × 144.1 + 107.2). [d] Measured by GPC against polystyrene standards with appropriate Mark–Houwink corrections for PLA in THF at 30 °C.[31] [e] Molecular weight data not determined.

higher monomer to PLA conversion and the general increase in PDI during polymerisation were consistent with detrimental chain-shortening transesterification side reactions competing with linear chain growth and resembled the poorer agreement seen in the catalyst loading experiments (Fig. 6) at lower loadings of amine ($[rac\text{-LA}]_0 : [BnNH_2]_0$).

Up to the saturation limit, adding more **4** to the polymerisation mixture resulted in a linear increase in $k_{app(Sr)}$ (Fig. 8, right), whereas M_n(GPC) showed no systematic dependence on $[\mathbf{4}]_0$ (Fig. 9, right), as expected. However, the data for when $[BnNH_2]_0 : [\mathbf{4}]_0 = 5 : 4.0$ or $5 : 5.0$, where the molar equivalents of Sr significantly exceeded $[BnNH_2]_0$ (*i.e.* the number of growing chains), showed increasingly poor agreement between measured and expected M_n (*e.g.*, M_n(calcd) = 10 250 g mol^{-1}, M_n(GPC) = 5570 g mol^{-1} for $[BnNH_2]_0 : [\mathbf{4}]_0 = 5 : 5.0$, entry 14, Table 3). Thus not only does an excess of metal sites yield no net increase in rate, but seems to increase the number of chain-shortening (probably transesterification) processes.

In a similar way, compound **2** was conveniently examined under the same conditions as **4** (see Fig. S4 and S5† of the ESI and Table 3). A second-order dependence in [*rac*-LA] was again observed along with a first-order dependence in $[\mathbf{2}]_0$, and a saturation limit was reached once the molar equiv. of calcium centres exceeded $[BnNH_2]_0$. The experimental rate of propagation (eqn (3)) is therefore proportional to $[rac\text{-LA}]^2[\mathbf{2}]_0$ as was also found for **4**, and $k_{p(Ca)}[BnNH_2]_0^c = 315(10)$ M^{-2} min^{-1}, suggesting that $k_{p(Ca)} \approx 1.7 \times k_{p(Sr)}$, assuming the rate dependence on $[BnNH_2]_0$ is the same in each case (*vide infra*).

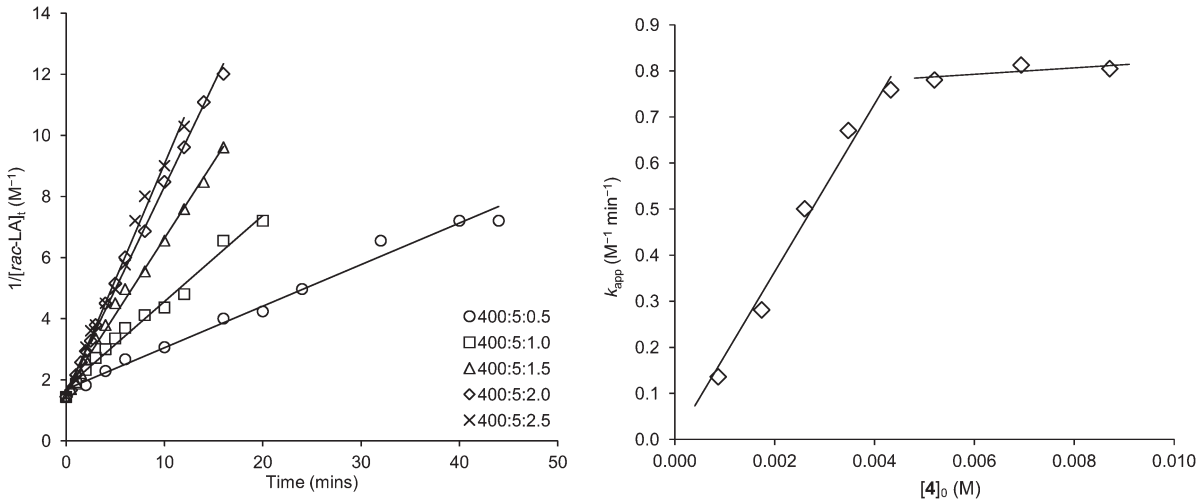

Fig. 8 Left: second-order plots of $1/[rac\text{-LA}]_t$ *vs.* time with increasing concentrations of $[\mathbf{4}]_0$. Rate constants, $k_{app(Sr)}$ = 0.136(5) (R^2 = 0.986), 0.281(11) (R^2 = 0.984), 0.501(11) (R^2 = 0.994), 0.671(11) (R^2 = 0.997) and 0.759(23) (R^2 = 0.991) M^{-1} min^{-1}. The vertical-axis intercepts of these plots are 1.68(13), 1.75(11), 1.63(8), 1.61(8) and 1.48(14) M^{-1} (expected value = $1/[rac\text{-LA}]_0$ = 1.44 M^{-1}). Right: plots of k_{app} *vs.* $[\mathbf{4}]_0$ for the polymerisation of *rac*-LA. $[rac\text{-LA}]_0 : [BnNH_2]_0$ = 400 : 5. Molar equiv. $[\mathbf{4}]_0$ = 0.5–2.5, 3.0, 4.0 or 5.0. $k_{p(Sr)}[BnNH_2]_0{}^c$ = 182(5) M^{-2} min^{-1} (R^2 = 0.983) based on $k_{app(Sr)}$ data in the range molar equiv. $[\mathbf{4}]_0$ = 0.5–2.5.

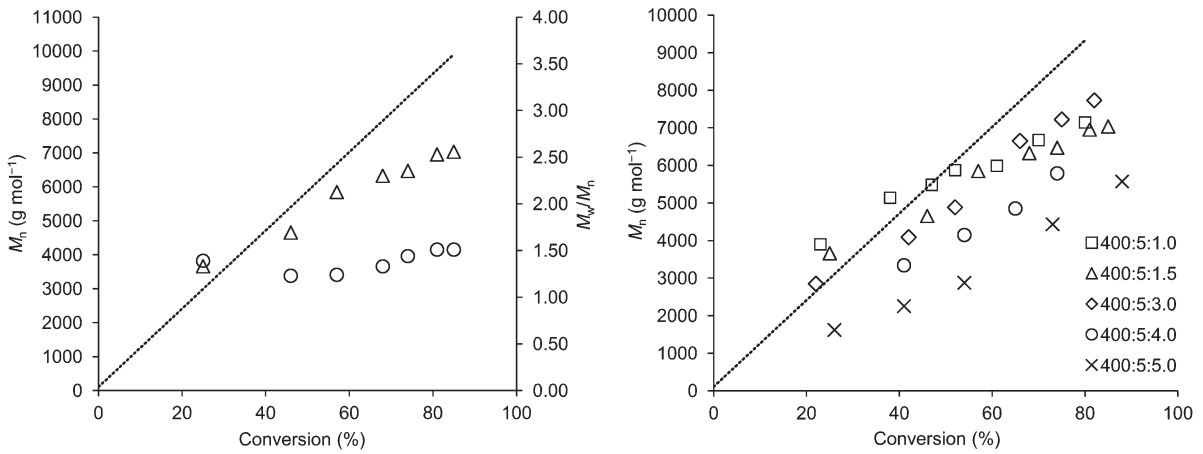

Fig. 9 Left: M_n(GPC) *vs.* conversion (triangles) and M_w/M_n *vs.* conversion (circles) plots for the run $[rac\text{-LA}]_0 : [BnNH_2]_0 : [\mathbf{4}]_0$ = 400 : 5 : 1.5. Right: M_n(GPC) *vs.* conversion plots for $[rac\text{-LA}]_0 : [\mathbf{4}]_0$ = 400 : 1.0, 1.5, 3.0, 4.0 or 5.0, $[rac\text{-LA}]_0 : [BnNH_2]_0$ = 400 : 5, PDIs = 1.4–1.7. The dashed lines represent M_n(calcd) based on $[rac\text{-LA}]_0 : [BnNH_2]_0$ = 400 : 5.

Kinetic studies: $BnNH_2$ dependence. From the preliminary experiments summarised in Table 2 it was clear that $BnNH_2$ had a significant effect on the rate of polymerisation (*cf.* entries 1, 2 and 5, and 3, 4 and 6), consistent in general terms with an activated monomer mechanism as inferred from the NMR tube scale experiments described above. To determine the order *c* with respect to $[BnNH_2]_0$ (*cf.* the rate expression proposed in eqn (3)), a ratio of $[rac\text{-LA}]_0 : [\mathbf{4}]_0$ = 400 : 1 was selected and held constant ($[rac\text{-LA}]_0$ = 0.69 M) while $[BnNH_2]_0$ was varied (Table 4, entries 8–11). $k_{app(Sr)}$ for the run $[rac\text{-LA}]_0 : [BnNH_2]_0 : [\mathbf{4}]_0$ = 400 : 5.0 : 1 has already been determined ($k_{app(Sr)}$ = 0.281(11) M^{-1} min^{-1}; entry 8, Table 3; reproduced for convenience as entry 9, Table 4). Doubling $[BnNH_2]_0$ to give $[rac\text{-LA}]_0 : [BnNH_2]_0 : [\mathbf{4}]_0$ = 400 : 10.0 : 1 gave $k_{app(Sr)}$ = 2.033(92) M^{-1} min^{-1} (Table 4, entry 11). This is considerably larger than for the 400 : 5.0 : 1 run, showing a non-linear dependence of rate (and thus $k_{app(Sr)}$) on $[BnNH_2]_0$. This fast rate (>90% conversion after 8 min) is at the upper limit of the practical reaction-sampling window and, so runs at 2.5 and 7.5 $BnNH_2$ molar equiv. were performed (entries 9 and 11, Table 4). The gradient of the line of least-squares fit (R^2 = 0.984) from the plot of $-\ln k_{app(Sr)}$ *vs.* $-\ln[BnNH_2]_0$ (Fig. 10, left) yielded an order (*c*) in $[BnNH_2]_0$ of 2.6(2).

A similar non-linear dependence of rate and $k_{app(Ca)}$ on $[BnNH_2]_0$ was found for **2**, but only for runs up to $[BnNH_2]_0 : [\mathbf{2}]_0$ = 7.5 (Table 4, entries 1–4). Holding $[rac\text{-LA}]_0$ and $[\mathbf{2}]_0$ constant at $[rac\text{-LA}]_0 : [BnNH_2]_0 : [\mathbf{2}]_0$ = 400 : 1 (as for **4**), the number of amine equiv. (*n*) were increased in the order 4.0, 5.0, 6.0, 7.5, 10.0 and 12.5 (Table 4). The use of 10 equiv. of $BnNH_2$ did not result in as great an increase in rate as expected based on the fitted line for 4.0–7.5 $BnNH_2$ equiv. (Fig. 10, right). The result was reproduced and a further point

Table 4 Apparent second-order rate constants ($k_{app(Ae)}$) and molecular weight data from the $[BnNH_2]_0$ dependence experiments for $[Ca_2(DBP)_4(DME)_4(\mu\text{-DME})]$ (**2**) and $[Sr_2(DBP)(\mu\text{-DBP})_3(DME)_3]$ (**4**)

Entry	Complex	$[rac\text{-LA}]_0 : [BnNH_2]_0 : [\mathbf{2}\text{ or }\mathbf{4}]_0$ [a]	$k_{app(Ae)}$ [b] (M^{-1} min^{-1})	R^2 [b]	Conv.[c] (%)	M_n (calcd)[c] (g mol^{-1})	M_n (GPC)[d] (g mol^{-1})	M_w/M_n [d]
1	**2**	400 : 4.0 : 1	0.285(6)	0.994	[e]	[e]	[e]	[e]
2	**2**	400 : 5.0 : 1	0.534(13)	0.997	87	10 140	8420	1.35
3	**2**	400 : 6.0 : 1	0.761(11)	0.998	[e]	[e]	[e]	[e]
4	**2**	400 : 7.5 : 1	1.264(33)	0.991	90	7030	8310	1.30
5	**2**	400 : 10.0 : 1	1.407(22)	0.997	85	5010	5950	1.42
6	**2**	400 : 10.0 : 1 (duplicate)	1.492(49)	0.987	[e]	[e]	[e]	[e]
7	**2**	400 : 12.5 : 1	1.891(58)	0.989	88	4170	4260	1.25
8	**4**	400 : 2.5 : 1	0.048(2)	0.976	[e]	[e]	[e]	[e]
9	**4**	400 : 5.0 : 1	0.281(11)	0.984	80	9330	7140	1.66
10	**4**	400 : 7.5 : 1	0.598(20)	0.984	87	6800	5900	1.70
12	**4**	400 : 10.0 : 1	2.033(92)	0.982	88	5180	5840	1.50

[a] $[rac\text{-LA}]_0 : [\mathbf{2}\text{ or }\mathbf{4}]_0$ = 400 : 1, $[rac\text{-LA}]_0$ = 0.69 M, THF, RT. [b] Apparent second-order rate constants ($k_{app(Ae)} = k_{p(Ae)}[\mathbf{2}\text{ or }\mathbf{4}]_0[BnNH_2]_0^c$) for consumption of *rac*-LA with standard error and R^2 determined by linear regression analysis. [c] Reactions monitored by ^1H NMR ($CDCl_3$). All quoted conversions refer to the last point where M_n(GPC) was determined. M_n(calcd) = (Conv. (%) × $[rac\text{-LA}]_0 : [BnNH_2]_0$ × 144.1 + 107.2). [d] Determined by GPC against polystyrene standards with appropriate Mark–Houwink corrections for PLA in THF at 30 °C.[31] [e] Molecular weight data not determined.

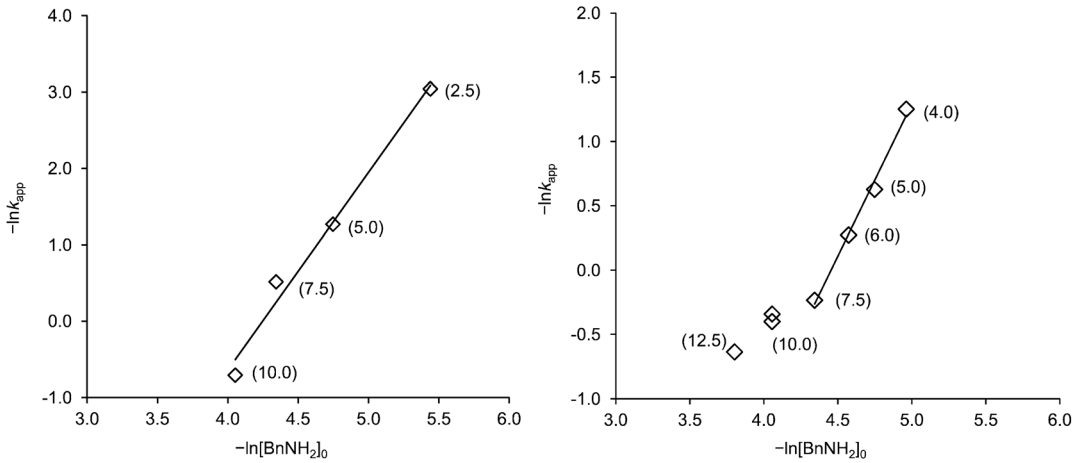

Fig. 10 $-\ln k_{app(Ae)}$ *vs.* $-\ln[BnNH_2]_0$ plots for $[Sr_2(DBP)(\mu\text{-DBP})_3(DME)_3]$ (**4**) (left) and $[Ca_2(DBP)_4(DME)_4(\mu\text{-DME})]$ (**2**) (right). The value in parentheses are number of amine equiv. (*n*) for the runs $[rac\text{-LA}]_0 : [BnNH_2]_0 : [Complex]_0 = 400 : n : 1$.

at 12.5 amine equiv. was likewise suggestive of a tendency to saturation, representing the rate of propagation becoming limited, presumably due to limitations of access to the smaller metal centre. An order (*c*) of 2.4(1) in $[BnNH_2]_0$ was calculated from the plot of $-\ln k_{app}$ *vs.* $-\ln[BnNH_2]_0$, based on the line of least-squares fit (R^2 = 0.993) through the points representing 4.0, 5.0, 6.0 and 7.5 $BnNH_2$ molar equiv. (Fig. 10, right).

Kinetic studies: concluding comments. In general terms, the observation that there is a rate dependence on both $[BnNH_2]_0$ (*i.e.* number of growing PLA chains) and $[\mathbf{2}\text{ or }\mathbf{4}]_0$ is consistent with an activated monomer mechanism,[2s,3b] as is the observation that the polymerisation rate only significantly increases with $[\mathbf{2}\text{ or }\mathbf{4}]_0$ while the number of metal centres is less than or equal to the number of growing chains (once each chain has a metal centre "partner" adding more catalyst has little positive effect and a kinetic saturation point is reached). However, the non-integer order dependence of $k_{app(Ae)}$ on $[BnNH_2]_0$ (*i.e.* on the concentration of growing polymer chains) for **2** and **4** is unexpected, but arises from identical kinetic behaviour for the two systems in the non-saturation region where $-\ln k_{app}$ *vs.* $-\ln[BnNH_2]_0$ is linear. Although the orders of 2.4(1) and 2.6(2) are individually close or equal to 2 (which is also the order in [*rac*-LA]) within three standard deviations, the fact that they are both independently closer to the average value of *ca.* 2.5 implies that this value may more likely be the correct interpretation. In combination with the first order dependence on $[\mathbf{2}\text{ or }\mathbf{4}]_0$ and second order *rac*-LA consumption the overall rate law therefore becomes $-d[rac\text{-LA}]/dt = k_{p(Ae)}[\mathbf{2}\text{ or }\mathbf{4}]_0[rac\text{-LA}]^2[BnNH_2]_0^{2.5}$.

This rate expression is clearly more complex than expected for a "simple" activated monomer mechanism.[2s] For example, Carpentier *et al.* found a rate expression $-d[L\text{-LA}]/dt = k_p[\text{complex}][L\text{-LA}][BnOH]$ for the BnOH co-initiated ROP of *L*-LA using cationic alkoxide or phenolate Ae (Ae = Mg, Ca, Sr, Ba) or Zn complexes.[3b] However, in these systems the supporting ligands are six-coordinate mixed aza-crown ether types, providing a

much better defined coordination environment than is possible for **2** and **4**. Scheme 2 and the solid state structure in Fig. 1–4 show the possible structural diversity available for the "Ae(DBP)$_2$" unit in presence of different donor ligands. Our NMR tube experiments between the macromonomer H-[*rac*-LA]$_{10}$-NHBn and [Sr$_2$(DBP)(μ-DBP)$_3$(DME)$_3$] (**4**) (Fig. S3† of the ESI) found that the polymer chain could act as a ligand by displacing DME. Therefore, while it is clear (*cf.* Fig. 8 and S4†) that each individual metal site in **2** and **4** is catalytically competent, the nature of the (one or more) complexes present under polymerisation conditions, and how any equilibria between them changes as a function of [*rac*-LA] or [BnNH$_2$]$_0$ (*i.e.* the concentration of PLA chains) cannot be known. Unusual fractional orders or orders greater than unity in ROP catalyst rate expressions have typically be attributed to solution equilibria and/or catalyst aggregation effects.[2q,35a,37]

Based on the $k_{p(Ae)}[BnNH_2]_0^{2.5}$ values of 182(5) M^{-2} min^{-1} (Ae = Sr, Fig. 8) and 315(10) M^{-2} min^{-1} (Ae = Ca, Fig. S4†) found for experiments with [BnNH$_2$]$_0$ = 8.6 × 10^{-3} M (Table 3) the propagation rate constants for $k_{p(Ca)}$ and $k_{p(Sr)}$ are *ca.* 4.6 × 10^7 and 2.6 × 10^7 $M^{-4.5}$ min^{-1}, respectively. This is also an unexpected result since previous studies for alkaline earth catalysts operating through the activated monomer mechanism[3b,12] found that k_p increased in the order Ae = Mg < Ca < Sr ≈ Ba. Further detailed kinetic studies of other systems will be needed to probe this aspect further, taking care that saturation kinetics are avoided both in terms of catalyst loading and metal : co-initiator ratios.

Synthesis and preliminary ROP studies of [Y(DBP)$_3$(THF)$_2$] (5)

The unusual experimental rate law for **2** and **4** and the identification of an activated monomer mechanism led us to consider again our previously reported[10] ROP results for the rare earth phenoxides [Ln(DBP)$_3$(THF)$_3$] (Ln = Nd or Gd). As mentioned the very fact ROP for these larger lanthanoids and their paramagnetic nature precluded detailed mechanistic studies of the type reported here for **2** and **4**. We therefore prepared the new diamagnetic compound [Y(DBP)$_3$(THF)$_2$] (**5**) by a protolysis reaction between [Y{N(SiHMe$_2$)$_2$}$_3$(THF)$_2$][38] and 3 equiv. of H-DBP in THF at RT (eqn (4)). The NMR, elemental analysis and other data are consistent with the structure shown in eqn (4) which is analogous to that of the starting complex [Y{N(SiHMe$_2$)$_2$}$_3$(THF)$_2$].

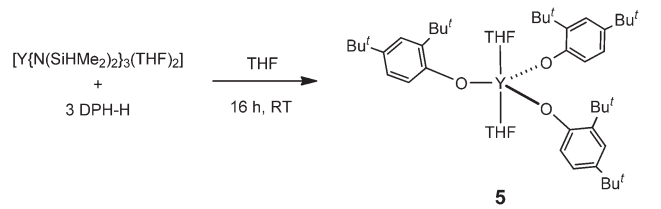

(4)

A detailed investigation of the ROP capability of **5** was beyond the scope of the present study but some preliminary experiments have been undertaken. Thus **5** was treated with 100 equiv. of *rac*-LA ([*rac*-LA]$_0$ = 0.69 M) in THF at RT in the absence of any co-initiator and then with 5 equiv. of BnOH and BnNH$_2$ respectively. In the reaction without any co-initiator, conversion of monomer to PLA was sluggish with 34% conversion being recorded after 30 min. At this point the catalyst was no longer active. The M_n(GPC) = 7460 g mol^{-1} was much higher than that calculated for even one chain per metal (M_n(calcd) = 4900 g mol^{-1}) and the PDI of 1.8 was comparable to values observed with **2**, **4** and [Ln(DBP)$_3$(THF)$_3$] (Ln = Nd or Gd). No –DBP end group was observed in the NMR or MALDI-ToF spectra, again as found for **2**, **4** and [Ln(DBP)$_3$(THF)$_3$].

The polymerisation performance improved when BnOH and BnNH$_2$ were included with [*rac*-LA]$_0$: [BnOH and BnNH$_2$]$_0$: [**5**]$_0$ = 100 : 5 : 1. In these cases ~95% conversion was achieved within 20 min in both cases. With BnOH the agreement between M_n(GPC) (2850 g mol^{-1}, BnOH) and M_n(calcd) (2880 g mol^{-1}) was consistent with one H-[PLA]-OBn polymer chain forming per equivalent of alcohol; likewise in the experiment with BnNH$_2$, M_n(GPC) = 3230 g mol^{-1} compared well with that expected (M_n(calcd) = 2890 g mol^{-1}). The PDIs of 1.2 (BnOH) and 1.3 (BnNH$_2$) were also consistent with well-controlled ROP processes, and the respective ^{1}H NMR and MALDI-ToF mass spectra featured –C(O)OBn and –C(O)NHBn end groups. However, as with [Ln(DBP)$_3$(THF)$_3$], **2** and **4** no heterotactic bias was detected and transesterification processes were shown to operate, given separation of Δ(m/z) = 72 g mol^{-1} between peak envelopes in the MALDI-ToF mass spectra.

Identical ^{1}H NMR tube scale studies to those for **2** and **4** were also performed with **5**. Treatment of **5** with 2–5 equiv. BnNH$_2$ or BnOH did not result in liberation of H-DBP. However, both BnNH$_2$ and BnOH were immediately consumed when 20 equiv. *rac*-LA was added to each mixture, forming H-[PLA]-NHBn and H-[PLA]-OBn, respectively. In neither case was free H-DBP observed. Therefore it would seem that this class of lanthanoid and group 3 tris(phenoxide) (and potentially others mentioned previously in the literature[11]) may behave in a similar manner to **2** and **4**, *i.e.*, proceeding *via* an activated monomer type propagation pathway. Further detailed studies will be required to develop this hypothesis further.

Conclusions

Four new alkaline earth complexes of the asymmetrically substituted 2,4-di-*tert*-butylphenol, namely [Ca(DBP)$_2$(THF)$_4$] (**1**), [Ca$_2$(DBP)$_4$(DME)$_4$(μ-DME)] (**2**), [Sr$_3$(μ-DBP)$_6$(THF)$_6$] (**3**), and [Sr$_2$(DBP)(μ-DBP)$_3$(DME)$_3$] (**4**) have been synthesised by RTP reactions and structurally characterised. The difference in ionic radii between Ca and Sr, coupled with the differing steric coordination numbers of THF compared to DME resulted in four distinct structural types. In addition the new yttrium compound [Y(DBP)$_3$(THF)$_3$] (**5**) was also synthesised by an amide-protolysis approach. While **2**, **4** and **5** are poor initiators for the ROP of lactide in their own right, addition of BnOH or BnNH$_2$ as co-initiators gave better controlled systems. This was the first example for a group 2 metal of amine co-initiated

ROP. The complex form of the rate expression, $-d[rac\text{-LA}]/dt = k_{p(Ae)}[\mathbf{2} \text{ or } \mathbf{4}]_0[rac\text{-LA}]^2[BnNH_2]_0^{2.5}$, differs from that described by Carpentier and Sarazin and most likely reflect the poorly-defined supporting ligand environment in the systems under consideration here.

Experimental

All products are air-sensitive and required the use of glove-box and Schlenk and vacuum line techniques, and were manipulated under a dinitrogen or argon atmosphere. Solvents were dried by distillation over sodium or sodium/benzophenone. All solvents were stored in J. Young Teflon valve ampoules. Elemental analyses (C, H) were performed by the Campbell Microanalytical Laboratory, University of Otago, Dunedin, New Zealand or by the Elemental Analysis Service at the London Metropolitan University. Infrared spectra were obtained as Nujol mulls with a Perkin Elmer 1600 FTIR or Perkin Elmer Spectrum RX1 instrument. ^{1}H, ^{13}C and ^{19}F NMR spectra were recorded on a Bruker DPX 300 MHz spectrometer, the former being referenced to residual protio-solvent peaks. Melting points were measured in pipettes sealed under dinitrogen, and are uncorrected. 2,4-Di-*tert*-butylphenol (H-DBP) was purchased from Sigma-Aldrich, and was not further purified. The compounds $[Y\{N(SiHMe_2)_2\}_3(THF)_2]$[38] and bis(pentafluorophenyl)mercury[39] were synthesised according to the published procedures. Calcium and strontium metals were purchased from Aldrich as chunks or turnings which were freshly filed under nitrogen prior to use.

MALDI-ToF MS analysis was performed on a Waters MALDI micro equipped with a 337 nm nitrogen laser and an accelerating voltage of 25 kV was applied. The polymer samples were dissolved in THF at a concentration of 1.0 mg mL^{-1}. The cationisation agent used was potassium trifluoroacetate (Fluka, >99%) dissolved in THF at a concentration of 5.0 mg mL^{-1}. The matrix used was *trans*-2-[3-(4-*tert*-butylphenyl)-2-methyl-2-propenylidene]-malononitrile (DCTB) (Fluka) and was dissolved in THF at a concentration of 40 mg mL^{-1}. Solutions of matrix, salt and polymer were mixed in a volume ratio of 4 : 1 : 4, respectively. The mixed solution was hand spotted on a stainless steel MALDI target and left to dry. The spectra were recorded in the reflectron mode.

Polymer molecular weights (M_w, M_n and PDI) were determined by GPC using a Polymer Laboratories PL-GPC50 Plus instrument equipped with a Polymer Laboratories Plgel Mixed-D column (300 mm length, 7.5 mm diameter) and a refractive index (RI) detector. Samples were dissolved in THF (Fisher, HPLC grade, stabilised with BHT, 2.5 ppm) at a concentration of 2.0 mg mL^{-1} and filtered prior to injection. THF (Fisher, HPLC grade, stabilised with BHT, 2.5 ppm) was used as the eluent at 30 °C and the flow rate was set to 1.0 mL min^{-1}. Linear polystyrenes (Polymer Laboratories) were used as the primary calibration standards and the appropriate Mark–Houwink corrections for PLA in THF at 30 °C were used to calculate the experimental molecular weights.[31]

$[Ca(DBP)_2(THF)_4]$ (1)

Calcium metal filings (0.20 g, 5.0 mmol), bis(pentafluorophenyl)mercury (0.55 g, 1.0 mmol), 2,4-di-*tert*-butylphenol (0.47 g, 2.3 mmol), and Hg metal (2 drops), were added to a Schlenk flask with dry THF (20 mL), and placed in an ultrasound bath for ~60 h. A pale yellow solution was observed. The solution was filtered and concentrated under vacuum to 6 mL and left to stand at −4 °C. Crystallisation was initiated when returned to room temperature, and small colourless crystals grew over 24 h. Yield = 0.65 g (76%), m.p. 76–80 °C. Anal. found (calcd for $C_{44}H_{74}CaO_6$): C, 71.37 (71.50); H, 9.84 (10.09) %. ^{1}H NMR (300.13 MHz, C_6D_6, 303 K): 7.44 (s, 2H, H3(Ar)), 7.18 (br s, 2H, H5(Ar)), 6.84 (br s, 2H, H6(Ar)), 3.47 (s, 16H, OCH_2CH_2), 1.62 (s, 18H, 2-Bu^t), 1.40 (s, 18H, 4-Bu^t), 1.30 (s, 16H, OCH_2CH_2). ^{13}C-{^{1}H} NMR (125.8 MHz, C_6D_6, 298 K): 160.8 (ArC_q-1), 137.1 and 136.5 (ArC_q-2 and ArC_q-4), 123.9 and 123.7 (ArC-5 and ArC-3), 121.1 (ArC-6), 68.3 (OCH_2CH_2), 35.4 (2-$C(CH_3)_3$), 34.2 (4-$C(CH_3)_3$), 32.3 (4-C(CH_3)$_3$), 31.0 (2-C(CH_3)$_3$), 25.5 (OCH_2CH_2) ppm. IR (Nujol mull): 1595 (s), 1404 (w), 1306 (m), 1256 (m), 1203 (m), 1141 (m), 1117 (m), 1074 (m), 1036 (m), 885 (m), 821 (m), 731 (m), 666 (m), 633 (m) cm^{-1}.

$[Ca_2(DBP)_4(DME)_4(\mu\text{-DME})]$ (2)

Calcium metal filings (0.25 g, 6.2 mmol), bis(pentafluorophenyl)mercury (0.55 g, 1.0 mmol), 2,4-di-*tert*-butylphenol (0.47 g, 2.3 mmol), and Hg metal (3 drops), were added to a Schlenk flask along with dry DME (30 mL). Upon sonication for 60 h, the pale yellow solution was filtered and concentrated under vacuum to 6 mL and left to stand at −4 °C. Small colourless crystals grew over one week. Yield = 0.43 g (55%), m.p. 160 °C, dec. temp. 220 °C. Anal. found (calcd for $C_{76}H_{134}Ca_2O_{14}$): C, 67.80 (67.51); H, 10.0 (9.99) %. ^{1}H NMR (300.13 MHz, C_6D_6, 303 K): 7.52 (s, 4H, H3(Ar)), 7.23 (d, ^3J = 6.0 Hz, 4H, H5(Ar)), 6.92 (d, ^3J = 6.0 Hz, 4H, H6(Ar)), 3.11 (s, 20H, CH_3OCH_2), 2.94 (s, 30H, CH_3OCH_2), 1.70 (s, 36H, 2-Bu^t), 1.40 (s, 36H, 4-Bu^t). ^{13}C NMR (125.80 MHz, C_6D_6, 298 K): 160.4, 137.8 and 136.4 (br, ArC_q-1,2,4), 124.0, 123.6 and 120.3(ArC-5,3,6), 70.7 (CH_3OCH_2), 59.7 (CH_3OCH_2), 35.3 and 34.1 ($C(CH_3)_3$), 32.1 and 30.5 (C(CH_3)$_3$). ^{1}H NMR (500.3 MHz, C_6D_6, 298 K): 7.50 (s, 4H, H3(Ar)), 7.20 (br s, 4H, H5(Ar)), 6.76 (br s, 4H, H6(Ar)), 2.81 (br s, 20H, CH_3OCH_2), 2.70 (br s, 30H, CH_3OCH_2), 1.66 (s, 36H, 2-Bu^t), 1.39 (s, 36H, 4-Bu^t) ppm. ^{13}C-{^{1}H} NMR (125.8 MHz, C_6D_6, 298 K): 160.4 (ArC_q-1), 137.8 and 136.4 (ArC_q-2 and ArC_q-4), 124.0 (ArC-5), 123.6 (ArC-3), 120.3 (ArC-6), 70.7 (CH_3OCH_2), 59.7 (CH_3OCH_2), 35.3 (2-$C(CH_3)_3$), 34.1 (4-$C(CH_3)_3$), 32.1 (4-C(CH_3)$_3$), 30.5 (2-C(CH_3)$_3$) ppm. IR (Nujol mull): 1598 (m), 1525 (w), 1307 (m), 1282 (m), 1202 (m), 1143 (m), 1115 (m), 1084 (w), 1070 (m), 1029 (w), 932 (w), 905 (w), 889 (w), 863 (w), 829 (w), 665 (w), 634 (w) cm^{-1}.

$[Sr_3(\mu\text{-DBP})_6(THF)_6]$ (3)

Strontium metal filings (0.90 g, 10.3 mmol), bis(pentafluorophenyl)mercury (0.56 g, 1.0 mmol), 2,4-di-*tert*-butylphenol (0.47 g, 2.3 mmol), and Hg metal (3 drops), were added to a Schlenk flask containing dry THF (20 mL), and ultrasonicated

for 3 d. The resulting yellow solution was filtered and concentrated under vacuum. Small rectangular block crystals suitable for X-ray crystallography grew over 2 d. Yield = 0.57g (77%), dec. temp. 150 °C. Anal. found (calcd for $C_{108}H_{174}O_{12}Sr_3$): C, 66.39 (67.30); H, 9.09 (9.10) %; the low %C found for **3** is attributed to partial loss of THF on drying *in vacuo*. ^{1}H NMR (300.13 MHz, C_6D_6, 303 K): 7.42 (s, 3H, ArH), 7.25 (s, overlapping, 9H, ArH), 6.75 (s, 3H, ArH), 5.79 (s, 3H, ArH), 3.43 (s, 24H, OCH_2CH$_2$), 1.54 (s, 27H, Bu^t), 1.41 and 1.39 (s, overlapping, 54H, Bu^t), 1.32 (s, 24H, OCH$_2$CH_2), 1.10 (s, 27H, Bu^t). ^{1}H NMR (300.13 MHz, C_6D_6, 343 K): 7.24 (s, 6H, H3(Ar)), 6.72 (br s, 6H, H5(Ar)), 5.73 (br s, 6H, H6(Ar)), 3.51 (s, 24H, OCH_2CH$_2$), 1.43 (s, 24H, OCH$_2$CH_2), 1.36 (s, 54H, 2-Bu^t), 1.09 (s, 54H, 4-Bu^t). ^{1}H NMR (300.13 MHz, THF-d$_8$, 303 K): 7.08 (s, 6H, H3(Ar)), 6.84 (d, 6H, H5(Ar)), 3.61 (m, THF, integration could not be determined owing to solvent resonance), 1.78 (m, THF, integration could not be determined owing to solvent resonance), 1.44 (s, 54H, 2-Bu^t), 1.24 (s, 54H, 4-Bu^t), H6 evidently broadened into baseline. ^{1}H NMR (300.13 MHz, THF-d$_8$, 333 K): 7.09 (s, 6H, H3(Ar)), 6.83 (d, 6H, H5(Ar)), 6.75 (vbr s, 6H, H6(Ar)), 3.61 (s, THF, integration could not be determined owing to solvent resonance), 1.76 (s, THF, integration could not be determined owing to solvent resonance), 1.44 (s, 54H, 2-Bu^t), 1.24 (s, 54H, 4-Bu^t). ^{13}C-{^{1}H} NMR (125.8 MHz, C_6D_6, 298 K): 159.6 (ArC$_q$-1, two overlapping), 138.6 (ArC$_q$-2 or ArC$_q$-4), 137.4 (ArC$_q$-2 and ArC$_q$-4, three overlapping), 125.3, 124.7 and 124.1 (ArC-3 and ArC-5, four resonances with two overlapping), 119.6 (ArC-6, two overlapping), 68.0 (O*C*H$_2$CH$_2$), 35.3 and 35.0 (2-*C*(CH$_3$)$_3$), 34.3 and 34.2 (4-*C*(CH$_3$)$_3$), 32.2 (4-C(*C*H$_3$)$_3$, two overlapping), 30.7 and 30.5 (2-C(*C*H$_3$)$_3$) and 25.5 (OCH$_2$*C*H$_2$) ppm. IR (Nujol mull): 1599 (m), 1401 (w), 1303 (w), 1269 (s), 1201 (m), 1151 (m), 1126 (w), 1072 (m), 1036 (m), 886 (w), 829 (m), 727 (m), 669 (w), 636 (w) cm^{-1}. Single crystals obtained from THF (unit cell similar to that of the benzene solvate) provided only a connectivity quality structure. Small crystals for a higher quality synchrotron structure determination, of composition **3**·C$_6$H$_6$ were grown from benzene.

[Sr$_2$(DBP)(μ-DBP)$_3$(DME)$_3$] (4)

Strontium metal filings (0.90 g, 10.3 mmol), bis(pentafluorophenyl)mercury (0.56 g, 1.0 mmol), 2,4-di-*tert*-butylphenol (0.47 g, 2.3 mmol), and Hg metal (~3 drops), were added to a Schlenk flask with dry DME (30 mL). Ultrasonication for 24 h, followed by filtration and concentration of the resulting pale yellow solution yielded large, colourless block crystals. Yield = 0.62g (85%), dec. temp. 260 °C. Anal. found (calcd for $C_{68}H_{114}O_{10}Sr_2$): C, 64.54 (64.47); H, 9.22 (9.07) %. ^{1}H NMR (300.13 MHz, C_6D_6, 303 K): 7.45 (s, 4H, H3(Ar)), 7.14 (br s, 4H, H5(Ar), 6.71 (br s, 4H, H6(Ar)), 2.98 (s, 12H, CH$_3$OCH_2), 2.79 (s, 18H, CH_3OCH$_2$), 1.59 (s, 36H, 2-Bu^t), 1.44 (s, 36H, 4-Bu^t). ^{1}H NMR (300.13 MHz, toluene-d$_8$, 193 K): 7.81, 7.64, 7.47(s, ArH), 3.18, 3.07, 2.61(br s, DME), 1.90, 1.80, 1.60, 1.53, 1.45 (br s, Bu^t). ^{1}H NMR (300.13 MHz, THF-d$_8$, 303 K): 7.07 (s, 4H, H3 (Ar)), 6.82 (d, 4H, H5(Ar)), 3.43 (s, 12H, CH$_3$OCH_2), 3.27 (s, 18H, CH_3OCH$_2$), 1.44 (s, 36H, 2-Bu^t), 1.24 (s, 36H, 4-Bu^t), H6 evidently broadened into baseline. ^{1}H NMR (300.13 MHz, THF-d$_8$, 333 K): 7.09 (s, 4H, H3(Ar)), 6.82 (d, 4H, H5(Ar)), 6.71 (vbr s, 4H, H6(Ar)), 3.43 (s, 12H, CH$_3$OCH_2), 3.27 (s, 18H, CH_3OCH$_2$), 1.44 (s, 36H, 2-Bu^t), 1.23 (s, 36H, 4-Bu^t). ^{13}C-{^{1}H} NMR (125.8 MHz, C_6D_6, 298 K): 162.8 (ArC$_q$-1), 137.3 and 136.3 (ArC$_q$-2 and ArC$_q$-4), 124.3 (ArC-3), 124.0 (ArC-5), 120.2 (ArC-6), 71.0 (CH$_3$O*C*H$_2$), 59.1 (*C*H$_3$OCH$_2$) 35.5 (2-*C*(CH$_3$)$_3$), 34.2 (4-*C*(CH$_3$)$_3$), 32.3 (4-C(*C*H$_3$)$_3$), 30.7 (2-C(*C*H$_3$)$_3$) ppm. IR (Nujol mull,): 1598 (s), 1525 (w), 1307 (m), 1272 (m), 1201 (m), 1146 (w), 1111 (w), 1084 (w), 1071 (m), 1016 (w), 925 (w), 907 (w), 887 (w), 856 (m), 830 (m), 667 (m), 638 (m) cm^{-1}.

Attempted synthesis of [Sr$_3$(DBP)$_6$(THF)$_6$] in the absence of Hg(C$_6$F$_5$)$_2$

Strontium metal filings (0.90 g, 10.3 mmol), 2,4-di-*tert*-butylphenol (0.47 g, 2.3 mmol), and Hg metal (3 drops), were added to a Schlenk flask containing dry THF (20 mL), and ultrasonicated for 3 d. The reaction mixture was filtered and concentrated to dryness under vacuum. Analysis of the bulk material by ^{1}H NMR and IR spectroscopy showed only starting materials.

[Y(DBP)$_3$(THF)$_2$] (5)

A solution of 2,4-di-*tert*-butylphenol (0.53 g, 2.54 mmol) in THF (10 mL) was added dropwise to a stirring solution of [Y{N(SiHMe$_2$)$_2$}$_3$(THF)$_2$] (0.53 g, 0.85 mmol) in THF (10 mL) at room temperature. The reaction mixture was stirred for 16 h, during which time the solution colour changed from colourless to yellow but remained clear. The volatiles were removed under reduced pressure and the crude solids were dissolved in THF (10 mL). The solution was filtered and then concentrated under reduced pressure. Hexanes were added (10 mL) and the title compound precipitated as a white solid, which was isolated by filtration and dried *in vacuo* at 0 °C. Yield = 0.40 g (56%). Anal. found (calcd for $C_{50}H_{79}O_5Y$): C, 70.56 (70.73); H, 9.29 (9.38)%. ^{1}H NMR (500.3 MHz, C_6D_6, 298 K): 7.60 (d, ^4J = 2.6 Hz), 3H, H3(Ar)), 7.35 (dd, ^3J = 8.4 Hz, ^4J = 2.6 Hz, 3H, H5 (Ar)), 7.13 (d, ^3J = 8.4 Hz, 3H, H6(Ar)), 3.73 (br s, 8H, OCH_2CH$_2$), 1.76 (s, 27H, 2-*Bu*^{t}), 1.38 (s, 27H, 4-*Bu*^{t}), 1.06 (br s, 8H, OCH$_2$CH_2) ppm. ^{13}C-{^{1}H} NMR (125.8 MHz, C_6D_6, 298 K): 161.3 (ArC$_q$-1), 138.2 (ArC$_q$-2), 135.9 (ArC$_q$-4), 123.9 (ArC-3), 123.4 (ArC-5), 121.8 (ArC-6), 68.0 (O*C*H$_2$CH$_2$), 35.5 (2-*C*(CH$_3$)$_3$), 34.3 (4-*C*(CH$_3$)$_3$), 32.1 (4-C(*C*H$_3$)$_3$), 30.5 (2-C(*C*H$_3$)$_3$), 25.7 (OCH$_2$*C*H$_2$) ppm. IR (Nujol mull): 1602 (w), 1485 (s), 1419 (m), 1361 (s), 1219 (m), 1203 (m), 1153 (w), 1086 (m), 1018 (m), 827(s), 742 (m) cm^{-1}.

Representative procedure for room temperature *rac*-LA polymerisations without a co-initiator

In a glove-box, *rac*-LA (0.20 g, 1.39 mmol, 100 equiv.) was weighed into a vial and dissolved in THF (1.5 mL). The monomer solution was added quickly in one portion to a stirring solution of [Ca$_2$(DBP)$_4$(DME)$_4$(μ-DME)] (**2**), [Sr$_3$(μ-DBP)$_6$-(THF)$_6$] (**3**), and [Sr$_2$(DBP)(μ-DBP)$_3$(DME)$_3$] (**4**) or [Y(DBP)$_3$-(THF)$_2$] (**5**) ([*rac*-LA]$_0$: [Complex]$_0$ = 100 : 1) in THF (0.5 mL). The vial was sealed and the reaction mixture stirred until high conversion was recorded, before immediate quenching outside

the glove-box by addition of THF (as supplied, ≈0.5 mL). Four aliquots (≈0.2 mL) were taken and dried *in vacuo*. These samples were used for ^{1}H NMR ($CDCl_3$), MALDI-ToF MS and GPC analysis.

Representative procedure for room temperature *rac*-LA polymerisations with co-initiators

In a glove-box, *rac*-LA (0.20 g, 1.39 mmol, 100 equiv.) was weighed into a vial and dissolved in THF (1.5 mL). The monomer solution was added quickly in one portion to a stirred mixture of $[Ca_2(DBP)_4(DME)_4(\mu\text{-DME})]$ (**2**), $[Sr_3(\mu\text{-DBP})_6(THF)_6]$ (**3**), and $[Sr_2(DBP)(\mu\text{-DBP})_3(DME)_3]$ (**4**) or $[Y(DBP)_3(THF)_2]$ (**5**) ($[rac\text{-LA}]_0 : [Complex]_0 = 100 : 1$) and co-initiator ($[Co\text{-initiator}]_0 : [Complex]_0 = 5 : 1$ in THF (0.5 mL). An appropriate volume of $BnNH_2$ or BnOH was measured using a Hamilton microlitre syringe. The vial was sealed and the reaction mixture stirred for 30 min before immediate quenching outside the glove-box by addition of THF (as supplied, ≈0.5 mL). Four aliquots (≈0.2 mL) were taken and dried *in vacuo*. These samples were used for ^{1}H NMR ($CDCl_3$), MALDI-ToF MS and GPC analysis.

Representative kinetics procedures for room temperature *rac*-LA polymerisations using $[Ca_2(DBP)_4(DME)_4(\mu\text{-DME})]$ (2) or$[Sr_2(DBP)(\mu\text{-DBP})_3(DME)_3]$ (4)

In a glove-box, *rac*-LA (0.80 g, 2.78 mmol, $[rac\text{-LA}]_0 : [Complex]_0 = 400 : 1.0–5.0$) was weighed into a vial and dissolved in THF (7.5 mL). The monomer solution was added quickly in one portion to a stirred mixture of **2** or **4** ($[rac\text{-LA}]_0 : [Complex]_0 = 400 : 1.0–5.0$) and co-initiator ($[BnNH_2]_0 : [Complex]_0 = 12.5 : 1$, $10.0 : 1$, $7.5 : 1$, $6.0 : 1$, $5.0 : 1$, $4.0 : 1$ or $2.5 : 1$ in THF (0.5 mL). An appropriate volume of $BnNH_2$ was measured using a Hamilton microlitre syringe. Aliqouts (≈0.1 mL) were taken at the appropriate time interval and were quenched inside the glove-box with degassed but not dried THF (6 drops). The volatiles were removed from the aliquots under reduced pressure and dried *in vacuo*. The crude aliquots were dissolved in $CDCl_3$ for determination of the monomer to polymer conversion by ^{1}H NMR analysis. The conversion was measured by integration of the C*H*(Me) resonances of PLA and unreacted *rac*-LA. Aliquots were then recovered for GPC and MALDI-ToF MS analysis.

X-ray structure determinations for 1–4

Intensity data were collected using an Enraf–Nonius KAPPA CCD (for **1**) or a Bruker X8 Apex II CCD (for **2** and **4**) at 123 K with Mo-K_α radiation (λ = 0.71073 Å) or the Australian Synchrotron MX1 beamline (for **3**) at 100 K with single wavelength (λ = 0.712 Å). Suitable crystals were immersed in viscous hydrocarbon oil and mounted on a glass fibre on the diffractometer or a cryoloop on the beamline. From KAPPA or Apex defractometers, psi and omega scans, N_t (total) reflections were measured and reduced to No. of unique reflections, with $F_o > 2\sigma(F_o)$ being considered observed. Data were initially processed and corrected for absorption using the programs DENZO[40] and SORTAV,[41] or the Bruker Apex II program suite.[42] With the MX1 beamline, data were collected using the Blue Ice[43] GUI and processed with the XDS[44] software package. The structures were solved using direct methods, and observed reflections were used in least squares refinement on F^2, with anisotropic displacement parameters refined for non-hydrogen atoms. Hydrogen atoms were constrained in calculated positions and refined with a riding model. Structure solutions and refinements were performed using the programs SHELXS-97[45] and SHELXL-97[46] through the graphical interface X-Seed,[47] which was also used to generate the Figures. Other details of the structure solution and refinements are given in the ESI† (CIF data). A full listing of atomic coordinates, bond lengths and angles and displacement parameters for all the structures have been deposited at the Cambridge Crystallographic Data Centre (CCDC 914477–914480).

Crystal data for **1**: $C_{44}H_{74}CaO_6$, M = 739.11, colourless block, 0.08 × 0.05 × 0.05 mm^3, monoclinic, space group $P2_1/c$ (No. 14), a = 9.778(2), b = 9.6717(19), c = 22.946(5) Å, β = 94.60(3)°, V = 2163.1(8) Å^3, Z = 2, D_c = 1.135 g cm^{-3}, $F000$ = 812, $2\theta_{max}$ = 55.0°, 19375 reflections collected, 4963 unique (R_{int} = 0.0750). Final *GooF* = 1.049, R_1 = 0.0477, wR_2 = 0.1230, R indices based on 3917 reflections with $I > 2\sigma(I)$ (refinement on F^2), 238 parameters, 0 restraints. Lp and absorption corrections applied, μ = 0.188 mm^{-1}.

Crystal data for **2**: $C_{76}H_{134}Ca_2O_{14}$, M = 1351.99, colourless block, 0.2 × 0.2 × 0.1 mm^3, monoclinic, space group $C2/c$ (No. 15), a = 24.136(3), b = 13.9781(14), c = 25.508(4) Å, β = 112.206(4)°, V = 7967.5(17) Å^3, Z = 4, D_c = 1.127 g cm^{-3}, $F000$ = 2968, $2\theta_{max}$ = 55.0°, 28504 reflections collected, 9130 unique (R_{int} = 0.0781). Final *GooF* = 1.069, R_1 = 0.0719, wR_2 = 0.1760, R indices based on 5273 reflections with $I > 2\sigma(I)$ (refinement on F^2), 432 parameters, 127 restraints. Lp and absorption corrections applied, μ = 0.200 mm^{-1}.

Crystal data for **3**·C_6H_6: $C_{114}H_{180}O_{12}Sr_3$, M = 2005.44, colourless block, 0.04 × 0.02 × 0.01 mm^3, trigonal, space group $R\bar{3}c$ (No. 167), a = 21.738(3), b = 21.738(3), c = 40.897(8) Å, γ = 120°, V = 16 737(5) Å^3, Z = 6, D_c = 1.194 g cm^{-3}, $F000$ = 6444, $2\theta_{max}$ = 50.0°, 68739 reflections collected, 3272 unique (R_{int} = 0.0561). Final *GooF* = 1.105, R_1 = 0.0519, wR_2 = 0.1237, R indices based on 3272 reflections with $I > 2\sigma(I)$ (refinement on F^2), 201 parameters, 24 restraints. Lp and absorption corrections applied, μ = 1.485 mm^{-1}.

Crystal data for **4**: $C_{68}H_{114}O_{10}Sr_2$, M = 1266.83, colourless block, 0.20 × 0.20 × 0.08 mm^3, monoclinic, space group $P2_1/n$ (No. 14), a = 16.312(3), b = 25.924(5), c = 16.982(3) Å, β = 96.27(3)°, V = 7138(2) Å^3, Z = 4, D_c = 1.179 g cm^{-3}, $F000$ = 2712, $2\theta_{max}$ = 55.0°, 50398 reflections collected, 16384 unique (R_{int} = 0.0935). Final *GooF* = 1.020, R_1 = 0.0560, wR_2 = 0.1197, R indices based on 10598 reflections with $I > 2\sigma(I)$ (refinement on F^2), 734 parameters, 0 restraints. Lp and absorption corrections applied, μ = 1.545 mm^{-1}.

Acknowledgements

We thank the Australian Research Council and the UK EPSRC and EU COST Action CM1006 for support. Aspects of this

research were undertaken on the MX1 beamline at the Australian Synchrotron, Victoria, Australia.

References

1 (*a*) E. Chiellini and R. Solaro, *Adv. Mater.*, 1996, **8**, 305; (*b*) K. E. Uhrich, S. M. Cannizzaro, R. S. Langer and K. M. Shakesheff, *Chem. Rev.*, 1999, **99**, 3181; (*c*) Y. Ikada and H. Tsuji, *Macromol. Rapid Commun.*, 2000, **21**, 117; (*d*) R. E. Drumright, P. R. Gruber and D. E. Henton, *Adv. Mater.*, 2000, **12**, 1841; (*e*) A.-C. Albertsson and I. K. Varma, *Biomacromolecules*, 2003, **4**, 1466; (*f*) R. Auras, B. Harte and S. Selke, *Macromol. Biosci.*, 2004, **4**, 835; (*g*) C. K. Williams and M. A. Hillmyer, *Polym. Rev.*, 2008, **48**, 1; (*h*) A. P. Dove, *Chem. Commun.*, 2008, 6446; (*i*) M. Kakuta, M. Hirata and Y. Kimura, *J. Macromol. Sci., Polym. Rev.*, 2009, **49**, 107; (*j*) E. S. Place, J. H. George, C. K. Williams and M. M. Stevens, *Chem. Soc. Rev.*, 2009, **38**, 1139.

2 (*a*) H. Keul and H. Hocker, *Macromol. Rapid Commun.*, 2000, **21**, 869; (*b*) M. Okada, *Prog. Polym. Sci.*, 2002, **27**, 87; (*c*) X. Lou, C. Detrembleur and C. Jérôme, *Macromol. Rapid Commun.*, 2003, **24**, 161; (*d*) S. Penczek, M. Cypryk, A. Duda, P. Kubisa and S. Slomkowski, *Prog. Polym. Sci.*, 2007, **32**, 247; (*e*) C. K. Williams, *Chem. Soc. Rev.*, 2007, **36**, 1573; (*f*) N. E. Kamber, W. Jeong, R. M. Waymouth, R. C. Pratt, B. G. G. Lohmeijer and J. L. Hedrick, *Chem. Rev.*, 2007, **107**, 5813; (*g*) D. Bourissou, S. Moebs-Sanchez and B. Martin-Vaca, *C. R. Chim.*, 2007, **10**, 775; (*h*) A.-C. Albertsson and R. K. Srivastava, *Adv. Drug Delivery Rev.*, 2008, **60**, 1077; (*i*) C. Jérôme and P. Lecomte, *Adv. Drug Delivery Rev.*, 2008, **60**, 1056; (*j*) M. Labet and W. Thielemans, *Chem. Soc. Rev.*, 2009, **38**, 3484; (*k*) H. Yasuda and E. Ihara, *Bull. Chem. Soc. Jpn.*, 1997, **70**, 1745; (*l*) B. J. O'Keefe, M. A. Hillmyer and W. B. Tolman, *J. Chem. Soc., Dalton Trans.*, 2001, 2215; (*m*) G. W. Coates, *J. Chem. Soc., Dalton Trans.*, 2002, 467; (*n*) O. Dechy-Cabaret, B. Martin-Vaca and D. Bourissou, *Chem. Rev.*, 2004, **104**, 6147; (*o*) J. Wu, T.-L. Yu, C.-T. Chen and C.-C. Lin, *Coord. Chem. Rev.*, 2006, **250**, 602; (*p*) A. Amgoune, C. M. Thomas and J.-F. Carpentier, *Pure Appl. Chem.*, 2007, **79**, 2013; (*q*) R. H. Platel, L. M. Hodgson and C. K. Williams, *Polym. Rev.*, 2008, **48**, 11; (*r*) C. A. Wheaton, P. G. Hayes and B. J. Ireland, *Dalton Trans.*, 2009, 4832; (*s*) N. Ajella, J.-F. Carpentier, C. Guillaume, S. M. Guillaume, M. Helou, V. Poirier, Y. Sarazin and A. A. Trifonov, *Dalton Trans.*, 2010, **39**, 8363; (*t*) M. J. Stanford and A. P. Dove, *Chem. Soc. Rev.*, 2010, **39**, 486; (*u*) I. dos Santos Vieira and S. Herres-Pawlis, *Eur. J. Inorg. Chem.*, 2012, 765.

3 (*a*) Y. Sarazin, V. Poirier, T. Roisnel and J.-F. Carpentier, *Eur. J. Inorg. Chem.*, 2010, 3423; (*b*) Y. Sarazin, B. Liu, T. Roisnel, L. Maron and J.-F. Carpentier, *J. Am. Chem. Soc.*, 2011, **133**, 9069.

4 (*a*) H. Y. Ma and J. Okuda, *Macromolecules*, 2005, **38**, 2665; (*b*) M. H. Chisholm and E. E. Delbridge, *New J. Chem.*, 2003, **27**, 1167; (*c*) H. D. Dyer, S. Huijser, N. Susperregui, F. Bonnet, A. D. Schwarz, R. Duchateau, L. Maron and P. Mountford, *Organometallics*, 2010, **29**, 3602.

5 O. Coulembier, M. K. Kiesewetter, A. Mason, P. Dubois, J. L. Hedrick and R. M. Waymouth, *Angew. Chem., Int. Ed.*, 2007, **46**, 4719.

6 Q. Cai, Y. Zhao, J. Bei, F. Xi and S. Wang, *Biomacromolecules*, 2003, **2003**, 828.

7 A. Kowalski, J. Libiszowski, T. Biela, M. Cypryk, A. Duda and S. Penczek, *Macromolecules*, 2005, **38**, 8170.

8 (*a*) L. Clark, M. G. Cushion, H. D. Dyer, A. D. Schwarz, R. Duchateau and P. Mountford, *Chem. Commun.*, 2010, **46**, 273; (*b*) L. Clark, D.Phil. Thesis, University of Oxford, 2012.

9 M. P. Blake, A. D. Schwarz and P. Mountford, *Organometallics*, 2011, **30**, 1202.

10 L. Clark, G. B. Deacon, C. M. Forsyth, P. C. Junk, P. Mountford and J. P. Townley, *Dalton Trans.*, 2010, **39**, 6693.

11 (*a*) W. M. Stevels, M. J. K. Ankoné, P. J. Dijkastra and J. Feijen, *Macromolecules*, 1996, **29**, 3332; (*b*) W. M. Stevels, M. J. K. Ankoné, P. J. Dijkastra and J. Feijen, *Macromolecules*, 1996, **29**, 6132; (*c*) C. Yu, L. Zhang, X. Ni, Z. Shen and K. Tu, *J. Polym. Sci., Part A: Polym. Chem.*, 2004, **42**, 6209.

12 H.-Y. Chen, L. Mialon, K. A. Abboud and S. A. Miller, *Organometallics*, 2012, **31**, 5252–5261.

13 (*a*) W. J. Evans and H. Katsumata, *Macromolecules*, 1994, **27**, 2330; (*b*) C. Iftner, F. Bonnet, F. Nief, M. Visseaux and L. Maron, *Organometallics*, 2011, **30**, 4482; (*c*) A. Momin, F. Bonnet, M. Visseaux, L. Maron, J. Takats, M. J. Ferguson, X.-F. Le Goff and F. Nief, *Chem. Commun.*, 2011, **47**, 12203.

14 R. D. Shannon, *Acta Crystallogr., Sect. A: Cryst. Phys., Diffr., Theor. Gen. Cryst.*, 1976, **32**, 751.

15 (*a*) T. P. Hanusa, in *Comprehensive Organometallic Chemistry III*, ed. R. H. Crabtree and D. M. P. Mingos, Elsevier, Oxford, 2007, vol. 2; (*b*) M. Westerhausen, M. Gärtner, R. Fischer and J. Langer, *Angew. Chem., Int. Ed.*, 2007, **46**, 1950; (*c*) M. Westerhausen, *Coord. Chem. Rev.*, 2008, **252**, 1516; (*d*) J. D. Smith, *Angew. Chem., Int. Ed.*, 2009, **48**, 6597; (*e*) A. G. M. Barrett, M. R. Crimmin, M. S. Hill and P. A. Procopiou, *Proc. R. Soc. London, Ser. A*, 2010, **466**, 927; (*f*) W. D. Buchanan, D. G. Allis and K. Ruhlandt-Senge, *Chem. Commun.*, 2010, **46**, 4449; (*g*) S. Harder, *Chem. Rev.*, 2010, **110**, 3852.

16 (*a*) M. H. Chisholm and N. W. Eilerts, *Chem. Commun.*, 1996, 853; (*b*) M. H. Chisholm, N. W. Eilerts, J. C. Huffman, S. S. Iyer, M. Pacold and K. Phomphrai, *J. Am. Chem. Soc.*, 2000, **122**, 11845; (*c*) B. M. Chamberlain, M. Cheng, D. R. Moore, T. M. Ovitt, E. Lobkovsky and G. W. Coates, *J. Am. Chem. Soc.*, 2001, **123**, 3229; (*d*) M. H. Chisholm, J. Gallucci and K. Phomphrai, *Chem. Commun.*, 2003, 48; (*e*) M. S. Hill and P. B. Hitchcock, *Chem. Commun.*, 2003, 1758; (*f*) M. Westerhausen, S. Schneiderbauer, A. N. Kneifel, Y. Söltl, P. Mayer, H. Nöth, Z. Zhong, P. J. Dijkastra and J. Feijen, *Eur. J. Inorg. Chem.*, 2003, 3432; (*g*) Z. Zhong, S. Schneiderbauer, P. J. Dijkastra,

M. Westerhausen and J. Feijen, *Polym. Bull.*, 2003, **51**, 175; (*h*) M. H. Chisholm, J. C. Gallucci and K. Phomphrai, *Inorg. Chem.*, 2004, **43**, 6717; (*i*) A. P. Dove, V. C. Gibson, E. L. Marshall, A. J. P. White and D. J. Williams, *Dalton Trans.*, 2004, 570; (*j*) M. H. Chisholm, J. C. Gallucci and K. Phomphrai, *Inorg. Chem.*, 2005, **44**, 8004; (*k*) T. Chivers, C. Fedorchuk and M. Parvez, *Organometallics*, 2005, **24**, 580; (*l*) J. Ejfler, M. Kobylka, L. B. Jerzykiewicz and P. Sobota, *Dalton Trans.*, 2005, 2047; (*m*) M. G. Davidson, C. T. O'Hara, M. D. Jones, C. G. Keir, M. F. Mahon and G. Kociok-Köhn, *Inorg. Chem.*, 2007, **46**, 7686; (*n*) V. Poirier, T. Roisnel, J.-F. Carpentier and Y. Sarazin, *Dalton Trans.*, 2009, 9820; (*o*) D. J. Darensbourg, W. Choi, O. Karroonnirun and N. Bhuvanesh, *Macromolecules*, 2008, **41**, 3493; (*p*) J. Ejfler, K. Krauzy-Dziedzic, S. Szafert, L. B. Jerzykiewicz and P. Sobota, *Eur. J. Inorg. Chem.*, 2010, 3602; (*q*) Y. Sarazin, D. Rosca, V. Poirier, T. Roisnel, A. Silvestru, L. Maron and J.-F. Carpentier, *Organometallics*, 2010, **29**, 6569; (*r*) M. G. Cushion and P. Mountford, *Chem. Commun.*, 2011, **47**, 2276; (*s*) V. Poirier, T. Roisnel, J.-F. Carpentier and Y. Sarazin, *Dalton Trans.*, 2011, **40**, 523; (*t*) B. Liu, V. Dorcet, L. Maron, J.-F. Carpentier and Y. Sarazin, *Eur. J. Inorg. Chem.*, 2012, 3023; (*u*) B. Liu, T. Roisnel, J. P. Guegan, J.-F. Carpentier and Y. Sarazin, *Chem.–Eur. J.*, 2012, **18**, 6289; (*v*) B. Liu, T. Roisnel and Y. Sarazin, *Inorg. Chim. Acta*, 2012, **380**, 2; (*w*) S. Marks, M. Kuzdrowska, P. W. Roesky, L. Annunziata, S. M. Guillaume and L. Maron, *ChemPlusChem*, 2012, **77**, 350; (*x*) R. A. Collins, J. Unruangsri and P. Mountford, *Dalton Trans.*, 2013, **42**, 759.

17 (*a*) D. C. Bradley, R. C. Mehrotra, I. P. Rothwell and A. Singh, *Alkoxo and Aryloxo Derivatives of Metals*, Academic Press, London, 2001; (*b*) M. N. Bochkarev, L. N. Zakharov and G. S. Kalinina, *Organoderivatives of the Rare Earth Elements*, Kluwer, Dordrecht, 1995; (*c*) S. A. Cotton, in *Comprehensive Coordination Chemistry II*, ed. J. A. McCleverty and T. J. Meyer, Elsevier, Oxford, 2004, vol. 3, ch. 3.2, p. 93.

18 (*a*) G. B. Deacon, G. D. Fallon, C. M. Forsyth, S. C. Harris, P. C. Junk, B. W. Skelton and A. H. White, *Dalton Trans.*, 2006, 802; (*b*) G. B. Deacon and C. M. Forsyth, *Inorganic Chemistry Highlights*, Wiley-VCH, 2002; (*c*) G. B. Deacon, C. M. Forsyth and S. Nickel, *J. Organomet. Chem.*, 2002, **647**, 50.

19 (*a*) H. Schumann, J. A. Meese-Marktscheffel and L. Esser, *Chem. Rev.*, 1995, **95**, 865; (*b*) F. T. Edelmann, in *Comprehensive Organometallic Chemistry II*, ed. G. Wilkinson, F. G. A. Stone and E. W. Abel, Pergamon, Oxford, 1995, vol. 4, ch. 2, p. 11; (*c*) R. Anwander, *Top. Organmet. Chem.*, 1999, **2**, 1; (*d*) R. C. Mehrotra, A. Singh and U. M. Tripathi, *Chem. Rev.*, 1991, **91**, 1287; (*e*) W. J. Evans, *New J. Chem.*, 1995, **19**, 525; (*f*) L. G. Hubert-Pfalzgraf, *Coord. Chem. Rev.*, 1998, **178**, 967.

20 J. Marcalo and A. P. de Matos, *Polyhedron*, 1989, **8**, 2431.

21 C. M. Forsyth and G. B. Deacon, *Organometallics*, 2000, **19**, 1205; G. B. Deacon and C. M. Forsyth, *Organometallics*, 2003, **22**, 1349.

22 J. Hitzbleck, Ph.D. Thesis, Syracuse University, Syracuse, NY, 2004; J. Hitzbleck, G. B. Deacon and K. Ruhlandt-Senge, unpublished results.

23 T. J. Boyle, B. A. Hernandez-Sanchez, C. M. Baros, L. N. Brewer and M. A. Rodriguez, *Chem. Mater.*, 2007, **19**, 2016.

24 (*a*) J. P. Dunne, M. Tacke, C. Selinke and D. Stalke, *Eur. J. Inorg. Chem.*, 2003, 1416; (*b*) W. D. Buchanan, M. A. Guino-o and K. Ruhlandt-Senge, *Inorg. Chem.*, 2010, **59**, 7144; (*c*) O. Michel, C. Meermann, K. W. Törnroos and R. Anwander, *Organometallics*, 2009, **28**, 4783.

25 (*a*) P. B. Hitchcock, M. F. Lappert, G. A. Lawless and B. Royo, *J. Chem. Soc., Chem. Commun.*, 1990, 1141; (*b*) K. F. Tesh, T. P. Hanusa, J. C. Huffman and C. J. Huffman, *Inorg. Chem.*, 1992, **31**, 5572.

26 G. Becker, M. Niemeyer, O. Mundt, W. Schwarz, M. Westerhausen, M. W. Ossberger, P. Mayer, H. Nöth, Z. Zhong, P. J. Dijkstra and J. Feijen, *Z. Anorg. Allg. Chem.*, 2004, **630**, 2605.

27 (*a*) W. J. Evans, W. G. McClelland, M. A. Greci and J. W. Ziller, *Eur. J. Solid State Inorg. Chem.*, 1996, **33**, 145; (*b*) G. B. Deacon, P. C. Junk and G. J. Moxey, *New J. Chem.*, 2010, **34**, 1731.

28 (*a*) G. B. Deacon, P. C. Junk, G. J. Moxey, M. A. Guino-o and K. Ruhlandt-Senge, *Dalton Trans.*, 2009, 4878; (*b*) W. J. Evans, M. A. Greci and J. W. Ziller, *Inorg. Chem.*, 2000, **39**, 3213; (*c*) G. B. Deacon, P. C. Junk and G. J. Moxey, *Chem.–Asian J.*, 2009, **4**, 1717.

29 (*a*) W. J. Evans, M. A. Greci and J. W. Ziller, *J. Chem. Soc., Chem. Commun.*, 1998, 2367; (*b*) G. B. Deacon, C. M. Forsyth and P. C. Junk, *J. Organomet. Chem.*, 2000, **607**, 112; (*c*) G. B. Deacon, C. M. Forsyth, P. C. Junk, B. W. Skelton and A. H. White, *Chem.–Eur. J.*, 1999, **5**, 1452.

30 G. B. Deacon, P. C. Junk, G. J. Moxey, K. Ruhlandt-Senge, C. St. Prix and M. F. Zuniga, *Chem.–Eur. J.*, 2009, **15**, 5503.

31 J. R. Dorgan, J. Janzen, D. M. Knauss, S. B. Hait, B. R. Limoges and M. H. Hutchinson, *J. Polym. Sci., Part B: Polym. Phys.*, 2005, **43**, 3100.

32 M. T. Zell, B. E. Padden, A. J. Paterick, K. A. M. Thakur, R. T. Kean, M. A. Hillmyer and E. J. Munson, *Macromolecules*, 2002, **35**, 7700.

33 J. March, *Advanced Organic Chemistry*, 4th edn, Wiley-Interscience, New York, 1992.

34 F. Bonnet, A. R. Cowley and P. Mountford, *Inorg. Chem.*, 2005, **44**, 9046.

35 (*a*) T. P. A. Cao, A. Buchard, X. F. Le Goff, A. Auffrant and C. K. Williams, *Inorg. Chem.*, 2012, **51**, 2157; (*b*) P. I. Binda and E. E. Delbridge, *Dalton Trans.*, 2007, 4685.

36 Although **4** can polymerise *rac*-LA in the absence of $BnNH_2$, the reaction is very slow (30 min to convert 51 equiv. with $[rac\text{-LA}]_0 : [\mathbf{4}]_0 = 400 : 4$ (= 100 : 1)) compared to when an amine or alcohol is present. To a first approximation, polymerisations reactions initiated by **4** (or **2**) alone may be neglected over the timescale of these experiments.

37 R. D. Köhn, Z. Pan, J. Sun and C. Liang, *Catal. Commun.*, 2003, **4**, 33.

38 R. Anwander, O. Runte, J. Eppinger, G. Gerstberger, E. Herdtweck and M. Speigler, *J. Chem. Soc., Dalton Trans.*, 1998, 847.
39 G. B. Deacon, J. E. Cosgriff, E. T. Lawrenz, C. M. Forsyth and D. L. Wilkinson, in *Synthetic Methods of Organometallic and Inorganic Chemistry*, ed. W. A. Herrmann, Theime, Stuttgart, 1997, vol. 6, p. 48.
40 Z. Otwinowski and W. Minor, *Methods Enzymol.*, 1997, **276**, 307.
41 R. H. Blessing, *Acta Crystallogr., Sect. A: Fundam. Crystallogr.*, 1995, **51**, 33.
42 *Apex II Version 2.1*, Bruker AXS Ltd., Madison, Wisconsin.
43 T. M. McPhillips, S. E. McPhillips, H. J. Chiu, A. E. Cohen, A. M. Deacon, P. J. Ellis, E. Garman, A. Gonzalez, N. K. Sauter, R. P. Phizackerley, S. M. Soltis and P. J. Kuhn, *J. Synchrotron Radiat.*, 2002, **9**, 401.
44 W. Kabsch, *J. Appl. Crystallogr.*, 1993, **26**, 795.
45 G. M. Sheldrick, *SHELXS-97 Program for crystal structure solution*, University of Gottingen, Germany, 1997.
46 G. M. Sheldrick, *SHELXL-97 Program for crystal structure refinement*, University of Gottingen, Germany, 1997.
47 L. J. Barbour, *J. Supramol. Chem.*, 2001, **1**, 189.